CHAPTER 2

PROPAGATION CHARACTERISTICS OF WIRELESS CHANNELS

2.0 INTRODUCTION

One of the major limitations on the performance of a mobile communication system is the attenuation undergone by the signal as it travels from the transmitter to the receiver (Gilb 1965, IEEE 1988, Deli 1985, Cheu 1998). The path the signal takes from the transmitter to the receiver may be line-of-sight (LOS), as shown in Figure 2.1, in which the case the signal loss may not be severe.

However, in a typical urban surrounding, the path between the transmitter and receiver is indirect and the signal reaches the receiver through the processes of reflection, diffraction, refraction, and scattering from buildings, structures, and other obstructions in the path (Jake 1974). These means of signal transmission are examples of non-line-of-sight (N-LOS) propagation mechanisms (Clar 1968). Reflection occurs when a propagating electromagnetic signal meets an object that is much larger than the signal's wavelength. This happens when the signal enters a building. Reflection may occur at the walls of the building, as shown in Figure 2.2. Note that depending on the angle of incidence and the impedance of the wall, reflection may or may not be accompanied by refraction.

Diffraction occurs when the surface encountered by the electromagnetic wave has irregularities such as sharp edges. This leads to bending of the wave, making it possible to receive the signal even when no direct path exists between the transmitter and the receiver, as shown in Figure 2.3.

Scattering occurs when the medium through which the electromagnetic wave propagates contains a large number of objects smaller than the wavelength. The wave is scattered in all directions, as shown in Figure 2.4. This happens when an electromagnetic wave passes through a medium containing vegetation, clouds, or street signs, for example.

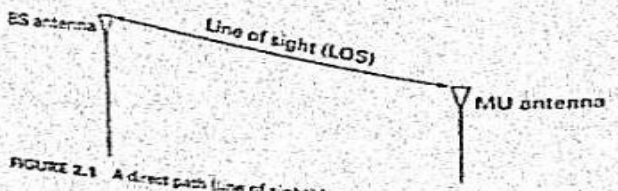

FIGURE 2.1 A direct path (line of sight) between two antennae.

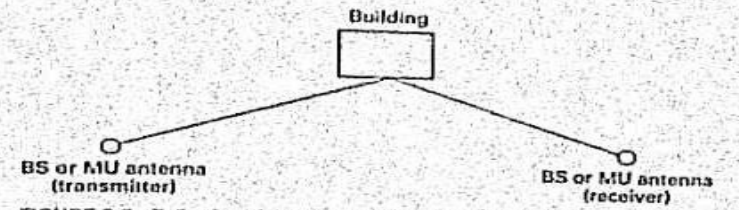

FIGURE 2.2 Reflection of the electromagnetic wave at a boundary.

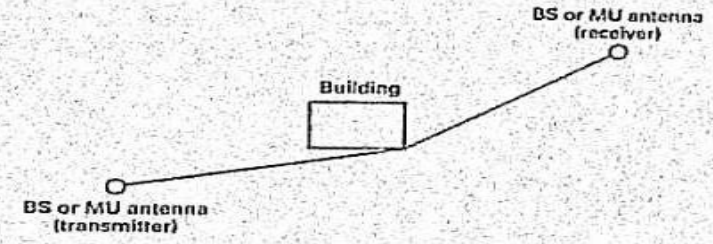

FIGURE 2.3 Diffraction of the electromagnetic wave at the edge of a building

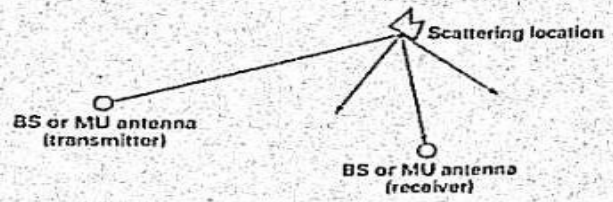

FIGURE 2.4 Scattering of the electromagnetic wave.

These non-line-of-sight (N-LOS) conditions (reflection, diffraction, and scattering) characterize most mobile communication transmissions. The free-space propagation models thus are not suited to calculate the attenuation undergone by the signal being received. The power detected by a receiver (MU or BS) is shown in Figure 2.5.

Observing the power at a separation of several kilometers, we see a steady decrease in power. This is the simple attenuation of power. It does not tell the whole story, however. If we zoom in to a distance of a couple of kilometers, we will see that the power fluctuates around a mean value and these fluctuations have a somewhat long period. This phenomenon is referred to as *long-term fading* or *large-scale fading*, and, as we shall see later, this can be described in terms of a *lognormal* distribution (Brau 1991, Bull 1977). If we zoom in further and examine the power over a few

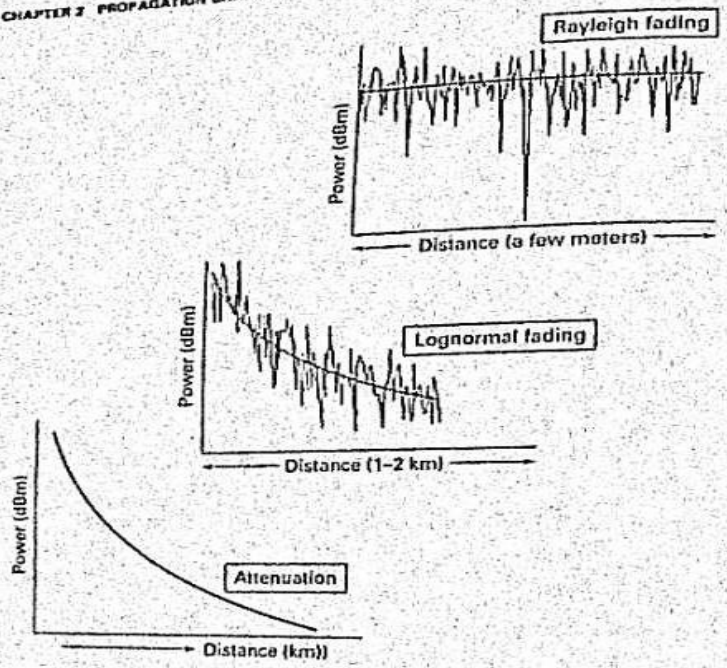

FIGURE 2.5 Power loss showing the three major effects: attenuation, long-term fading, and short-term fading.

hundred meters, we will see that the power is fluctuating more rapidly. The phenomenon giving rise to these fluctuations is referred to as *short-term fading* or *small-scale fading*, which, as we shall see later, can be described in terms of the *Rayleigh* distribution. We can thus see that the nature of the received signal is more complex than a simple description based on attenuation alone (Auli 1979, Akki 1994, Samp 1997). We will now look at these three phenomena associated with the propagation of wireless signals in greater detail.

2.1 ATTENUATION

Consider a very simple case where there is a direct path between the transmitter and receiver, as shown in Figure 2.6. In the absence of substantial obstacles in the path of the signal, the received signal power, P_r, follows the inverse square law (Gilb 1965, Jake 1974):

$$P_r \propto d^{-2}, \tag{2.1}$$

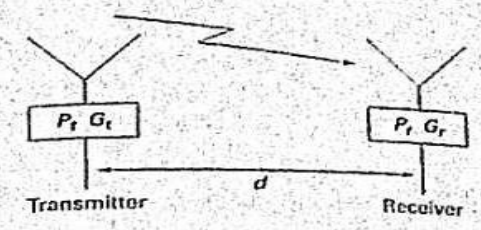

FIGURE 2.6 Free space propagation geometry.

with d being the distance between the transmitter and the receiver. The received power, $P_r(d)$, is normally expressed as

$$P_r(d) = \frac{P_t G_r G_t \lambda^2}{(4\pi)^2 d^2 L}, \quad d > 0, \tag{2.2}$$

The parameters G_t and G_r are the transmitter and receiver gains, respectively (Jake 1974). The operating wavelength is λ, and $L (\geq 1)$ represents any additional losses in the system not related to propagation losses, such as filter losses and antenna loss, etc. (i.e., hardware losses).

The transmitted power is P_t, in milliwatts. The product $P_t G_t$ is referred to as the *equivalent isotropic radiated power* (EIRP). Another parameter of interest is the *free-space* loss, L_{free}, given by

$$L_{free} = -20 \log_{10}\left(\frac{\lambda}{4\pi d}\right) \text{dB}. \tag{2.3}$$

The expression for EIRP can be used to estimate the received power at any distance from the transmitter using eq. (2.2),

$$P_r(d) = P_r(d_{ref})\left(\frac{d_{ref}}{d}\right)^2, \tag{2.4}$$

where d_{ref} is a reference distance. The reference distance must be smaller than the typical distances encountered in wireless communication systems and must fall in the far-field region of the antenna, so that losses beyond that point are purely distance-dependent effects (Rapp 1996b, Pahl 1995). This value is typically in the range of 100–1000 m. The power at a distance of d_{ref}, $P_r(d_{ref})$, is again in milliwatts. Making use of this approach, eq. (2.4) can be written as

$$P_r(d)\,\text{dBm} = 10\log_{10}[P_r(d_{ref})] + 20\log_{10}\left[\frac{d_{ref}}{d}\right]. \tag{2.5}$$

The actual loss suffered by signal at a frequency of f_0 (MHz) at a distance d (km) under the conditions of a flat, obstruction-free terrain, L_{free}, can also be obtained by rewriting the free-space propagation loss given in eq. (2.3):

$$L_{free} = -20 \log_{10}\left(\frac{c/f}{4\pi d}\right) \text{dB}, \tag{2.6}$$

where c is the free-space velocity of the electromagnetic wave, equal to 3×10^8 m/s, and f is the frequency. Expressing the frequency in megahertz, eq. (2.6) can now be expressed as

$$L_{free} = 32.44 + 20 \log_{10}(f) + 20 \log_{10}(d), \tag{2.7}$$

where d must be larger than 1 km, f is in megahertz, and d is in kilometers.

EXAMPLE 2.1

Consider an antenna transmitting a power of 10 W at 900 MHz. Calculate the received power at a distance of 2 km if propagation is taking place in free space.

Answer The wavelength at 900 MHz is $3c^8/9c^6 = (1/3)$ m. Using eq. (2.2) with $L_s = 1$, $G_t = G_r = 1$, and $d_{ref} = 100$ m, the received power at d_{ref} is

$$\frac{10}{(4\pi)^2}\left(\frac{1}{3 \times 100}\right)^2 = 0.7\,\mu\text{W}$$

or -31.5 dBm. Now, using eq. (2.4), the power at a distance of 2 km is -57.5 dBm. Using eq. (2.6), the loss is $32.44 + 20 \log_{10}(900) + 20 \log_{10}(2) = 97.5$ dB. Therefore, the received power is $10 \log_{10}(10^4) - 97.5 = -57.5$ dBm. □

The case of free-space propagation discussed above, of course, is an ideal case, and the power often attenuates at a rate much higher than predicted by the inverse square law. Hence, the loss experienced in most cases will be considerably higher (Rapp 1995, Deli 1985). It is possible to explore whether, instead of the power decreasing as the inverse of the square of the distance from the transmitter, the power loss follows an exponent of a higher order, ν, so that the received power P_r can be expressed as

$$P_r \propto d^{-\nu}, \tag{2.8}$$

where the loss parameter, ν, has a minimum value of 2 in free space and takes a value larger than 2 when free-space propagation conditions do not exist. The received power under non-line-of-sight (N-LOS) conditions can now be written by combining equations (2.4) and (2.8) as

$$P_r(d)\,\text{dBm} = 10 \log_{10}[P_r(d_{ref})] + 10\nu \log_{10}\left[\frac{d_{ref}}{d}\right], \tag{2.9}$$

where d_{ref} is the reference distance (100 m). Typical plots of the received power for a few different values of ν are shown in Figure 2.7, indicating that losses tend to grow when N-LOS conditions prevail. The higher values of ν correspond to city and urban areas, and lower values of ν correspond to suburban or rural areas.

EXAMPLE 2.2

In Example 2.1, calculate the received power in dBm if the loss parameter ν is 2.5, 3, and 4.

Answer The power at a short distance ($d_{ref} = 100$ m) is obtained from eq. (2.2) as -31.5 dBm. Now, using eq. (2.9), the power at a distance of 2 km is

-64 dBm for $\nu = 2.5$
-70.5 dBm for $\nu = 3$
-83.5 dBm for $\nu = 4$

□

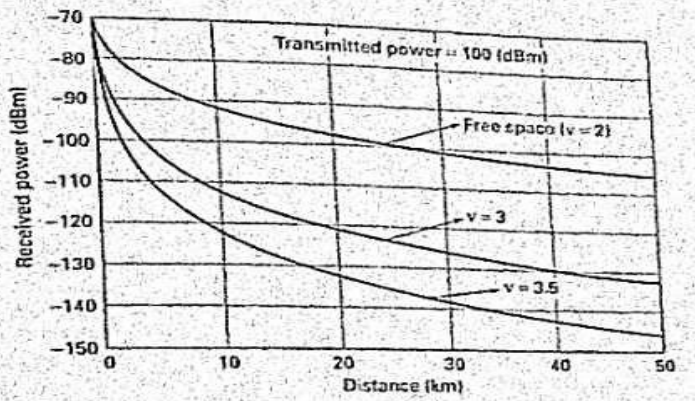

FIGURE 2.7 Received power for different values of loss parameter ν ($\nu = 2$ corresponds to free space). Increased loss is seen as ν goes up.

A number of models have been proposed to predict the loss of a signal as it travels to the receiver. These loss models combine empirical measurements in many cities and some physical models to account for the different ways in which radio-frequency signals travel. As mentioned earlier, the signals from the transmitter are reflected, scattered, refracted, diffracted, and absorbed by the terrain, which consists of buildings, vegetation, and other ground effects, before they reach the receiver. These various physical phenomena combine to produce significant attenuation in the signal. The loss of power is often accompanied by fluctuations, as shown in Figure 2.5, in the mean or median value of the power received, making predictions of received power (and design considerations based on received power) a little bit more difficult. A few different modes of transmission and reception of wireless signals (Meli 1993, Mehr 1999) are shown in Figures 2.8, 2.9, and 2.10.

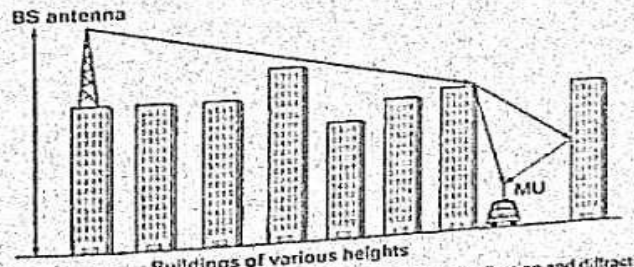

FIGURE 2.8 The signal reaches the receiver through reflection and diffraction.

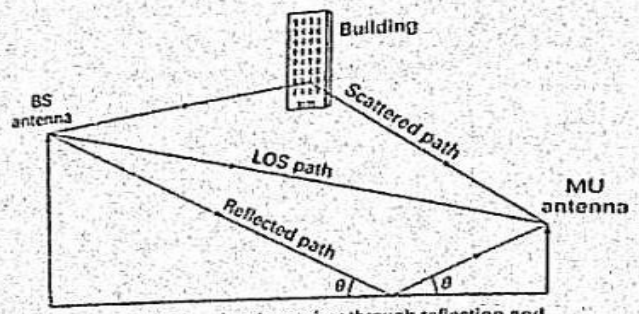

FIGURE 2.9 The signal reaches the receiver through reflection and scattering, as well as via a direct path.

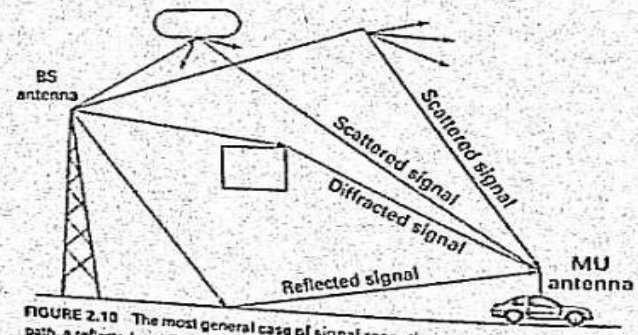

FIGURE 2.10 The most general case of signal reception, consisting of a direct path, a reflected path, a scattered path, and a diffracted path.

In Figure 2.8 the signal from the BS can reach the MU through the processes of diffraction and reflection. This is one of the common ways in which the transmission/reception of signals takes place in a city with tall buildings. In Figure 2.9 the signal from the BS takes three separate paths to reach the MU. In addition to the line-of-sight path, a path is provided by ground reflection and another path is provided by scattering from the building. The most general case is shown in Figure 2.10. In this case, the signal reaches the MU after undergoing reflection, scattering, diffraction, and possibly refraction after interaction with different structures in its path, or what may be described as "terrain-dependent" effects.

Combining all these different ways in which the signal can reach the receiver, Okumura and colleagues proposed a model to predict the median signal loss based on measurements conducted in and around Tokyo (Okum 1968). The model is based on the premise that it is possible to calculate the free-space loss between any two points for a base station antenna height of 200 m and a mobile antenna height of 3 m, with correction factors added to account for the terrain. Additional correction factors can be included

to account for other factors, such as street orientation. These correction factors take into account the following features, among others:

Antenna heights and transmission frequency (or wavelength)
Suburban, quasi-open space; hilly terrain; etc.
Diffraction loss due to mountains
Lakes
Road shape

Even though this model is very reasonable in predicting the signal loss, it is not easy to use since correction factors must be incorporated for every conceivable scenario, or the results will have to be extrapolated. To overcome some of these problems, Hata proposed a reasonably simple model that fits Okumura's graphical results (Hata 1980, 1985). Another model that provides for transmission loss is Lee's model (Lee 1980, 1993, 1997).

Note that the Hata model and Lee's model merely provide a formula for path loss with respect to distance. But path loss alone is not sufficient to characterize the channel through which the signal is traveling. A typical path loss observed (Figure 2.5) shows the effects of fading, both long-term and short-term.

Before examining the relationship between attenuation and fading, we will look at the Hata model as well as Lee's model for calculating the propagation loss. We will also look at the differences between indoor and outdoor propagation, and examine ways of modeling and calculating indoor propagation losses.

2.1.1 Hata Model

The Hata model (Hata 1980) is a significant improvement over Okumura's model (Okum 1968) for the prediction of propagation losses. The propagation in different geographical regions is taken into consideration using correction factors that have been empirically derived. The starting point in the loss prediction is the propagation in an urban area. The loss models are generally given in terms of the median loss rather than the mean loss. The losses are given in terms of the effective height (h_b) of the BS antenna and the height (h_{mu}) of the MU antenna (measured above the ground). The approach for estimating the effective height of the BS antenna is shown in Figure 2.11. Typically, BS

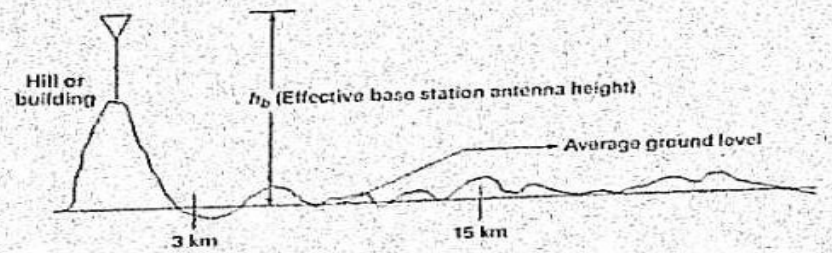

FIGURE 2.11 The effective height of the BS antenna.

antennae are mounted on top of existing buildings or other tall structures. Between 3 and 15 km from the base of the antenna to the MU antenna, the effective height is estimated to be above the average level of the terrain, as shown in the figure.

In the Hata model, median path loss, L_p (dB), in urban areas is given by

$$L_p\,(\text{dB}) = 69.55 + 26.16\,\log_{10}(f_0) + (44.9 - 6.55\,\log_{10}h_b)\log_{10}d - 13.82\,\log_{10}h_b - a(h_{ms}), \tag{2.10}$$

where

f_0 = carrier frequency (MHz)

d = separation between base station and mobile unit (km)

h_b = height of the base station antenna (m)

h_{ms} = height of the mobile unit antenna (m)

$a(h_{ms})$ = correction factor for mobile unit antenna height.

For large cities, the correction factor $a(h_{ms})$ is given by

$$a(h_{ms}) = 3.2\{\log_{10}(11.75h_{ms})\}^2 - 4.97 \quad (f_0 \geq 400\ \text{MHz}). \tag{2.11}$$

For small and medium cities, the correction factor is

$$a(h_{ms}) = \{1.1\,\log_{10}(f_0) - 0.7\}h_{ms} - \{1.56\,\log_{10}(f_0) - 0.8\}. \tag{2.12}$$

For suburban areas, the median loss, L_{sub}, is given by

$$L_{sub}\,(\text{dB}) = L_p - 2\left[\log_{10}\left(\frac{f_0}{28}\right)\right]^2 - 5.4, \tag{2.13}$$

where L_p is the median loss in small-to-medium cities. For rural areas, the median loss, L_{rur}, is given by

$$L_{rur}\,(\text{dB}) = L_p - 4.78\{\log_{10}(f_0)\}^2 + 18.33\,\log_{10}f_0 - 40.94, \tag{2.14}$$

where L_p is the median loss in small-to-medium cities. The only limitation of the Hata model is the requirement that the distance, d, between the BS and MU exceed 1 km.

The typical loss as given by the Hata model is shown in Figure 2.12. Note that the difference in correction factors between a large and a medium-to-small city is only about 1 dB. This makes the loss curves for these two cases appear to be very close.

The Hata model can also be used to estimate the value of the loss parameter ν. The received power, $P_r(d)$ (dBm), for any separation, d (km), between MU and BS can be expressed as

$$P_r(d)(\text{dBm}) = P_t - P_{L_{sm}}(d), \tag{2.15}$$

where P_t (dBm) is the transmitted power and $P_{L_{sm}}(d)$ is the loss calculated from Hata's model. The received power can also be expressed as

$$P_r(d) \propto \left(\frac{1}{d}\right)^{\nu}, \tag{2.16}$$

where ν is the path loss exponent.

The loss at the two distances d_{ref} and d (>1 km) can be expressed as

$$P_{L_{sm}}(d_{ref}) \propto 10\nu\,\log_{10}(d_{ref}) \tag{2.17}$$

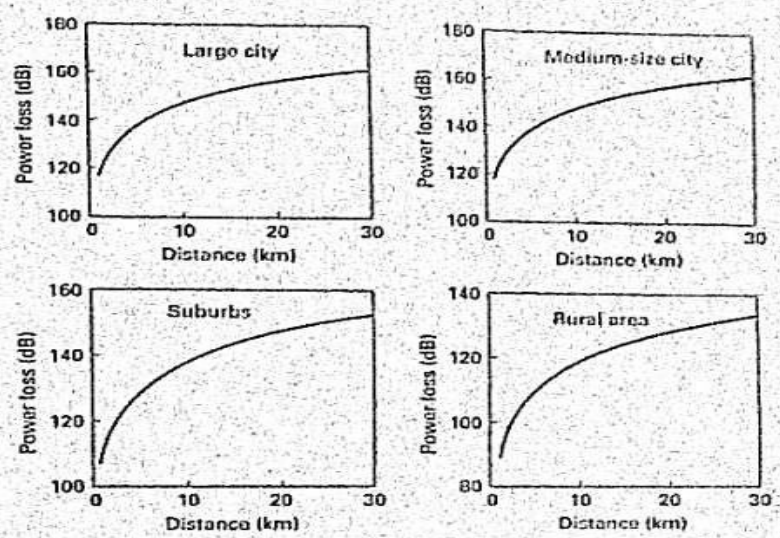

FIGURE 2.12 Loss calculations based on the Hata model for four different environments. Carrier frequency = 900 MHz, base station antenna height = 150 m, MU antenna height = 1.5 m.

and

$$P_{L_{sm}}(d) \propto 10\nu\,\log_{10}(d), \tag{2.18}$$

and the expression for ν becomes

$$\nu = \frac{P_{L_{sm}}(d) - P_{L_{sm}}(d_{ref})}{10[\log_{10}(d) - \log_{10}(d_{ref})]}, \tag{2.19}$$

where d_{ref} is 100 m and $P_{L_{sm}}$ is given by

$$P_{L_{sm}}(d_{ref}) = 10\,\log_{10}\left[\frac{(4\pi d_{ref})^2}{\lambda^2}\right], \tag{2.20}$$

obtained from eq. (2.2).

EXAMPLE 2.3

Find approximate values of the loss parameter, ν, using the Hata model for the four geographical regions: large city, small-to-medium city, suburb, and rural area.

Answer Using Figure 2.12, the loss values at a distance of 5 km are 131.36 dB, 131.34 dB, 121.40 dB, and 102.8 dB, respectively, for large city, small-to-medium city, suburb, and rural area. Using eq. (2.19), the respective values of ν are 4.05, 4.04, 3.3, and 2.11. Note that these values are approximate, and d must be 2 km or more to get reasonably stable values of ν. □

Extension of Hata Model to PCS The attenuation model proposed by Hata can be extended to PCS (personal communication system) environments (Meli 1993, Rapp 1996b, Garg 1997, Saun 1999). The median loss in urban areas, L_p (dB), can be expressed as

$$L_p(\text{dB}) = 46.3 + 33.93\log_{10}(f_0) - 13.82\log_{10}(h_b) - a(h_{\text{mu}}) + [44.9 - 6.55\log_{10}(h_b)]\log_{10} d + \text{Corr} \tag{2.21}$$

where Corr is the additional correction factor given by

$$\text{Corr} = \begin{cases} 0 \text{ dB for medium city and suburban areas} \\ 3 \text{ dB for metropolitan areas} \end{cases} \tag{2.22}$$

This model is valid for the following parameters only:

f_0: 1500–2000 MHz
h_b: 30–200 m
h_{mu}: 1–10 m
d: 1–20 km

The Hata model is applicable only for distances beyond 1 km, and thus cannot be used in microcells (see Chapter 4), where the distance between the transmitter and receiver may be only a few hundred meters. Newer models (the Har, Xia, and Bertoni model; and the Walfisch-Ikegami model) are available for loss prediction over short ranges, and are discussed in Section C.2 in Appendix C.

2.1.2 Lee's Model

Another model available for the prediction of path loss is the one proposed by Lee (Lee 1980, 1993). Based on measurements taken in three cities, including Philadelphia, the model provides the loss in signal strength on an area-to-area basis. These loss values can then be used as a set of initial values to get a point-to-point loss prediction. The median loss (area-to-area) at a distance d (km), $L(d)$, can be expressed as

$$L(d)(\text{dB}) = L_0 + 10\,\nu\log_{10}(d) + \alpha_c, \tag{2.23}$$

where L_0 is the loss at 1 km, ν is the loss parameter, and α_c is a correction factor. The predictions were done for a carrier frequency of 900 MHz, a transmitting (BS) antenna of height 30.5 m, and a receiving antenna height of 3 m. The correction factor, α_c, is included to account for any change in the standard parameters used in the model and can be expressed as

$$\alpha_c = 10\log_{10}(F), \tag{2.24}$$

The parameter F is the product of various correction factors,

where

$$F = F_1F_2F_3F_4F_5, \tag{2.25}$$

$$F_1 = \left[\frac{\text{actual base station antenna height (m)}}{30.5}\right]^2 \tag{2.26a}$$

$$F_2 = \left[\frac{\text{actual transmitted power (W)}}{10}\right] \tag{2.26b}$$

$$F_3 = \left[\frac{\text{actual gain of base station antenna}}{4}\right] \tag{2.26c}$$

$$F_4 = \left[\frac{\text{actual mobile unit antenna height (m)}}{3}\right]^2, \quad \text{height} \geq 3 \text{ m} \tag{2.26d}$$

F_5 = differential antenna gain correction factor at the mobile unit. (2.26e)

The loss based on the point-to-point model, $L_p(d)$, can now be expressed as

$$L_p(d)\,(\text{dB}) = L(d) + 20\log_{10}\left(\frac{h_{\text{eff}}}{10}\right), \tag{2.27}$$

where h_{eff} is the effective height of the antenna, taking into account the location of the antenna in relation to the terrain, as shown in Figure 2.13.

Note that the Hata model is easier than most of the other models for predicting propagation losses and will be used for the computation of the cell radius in Chapter 4.

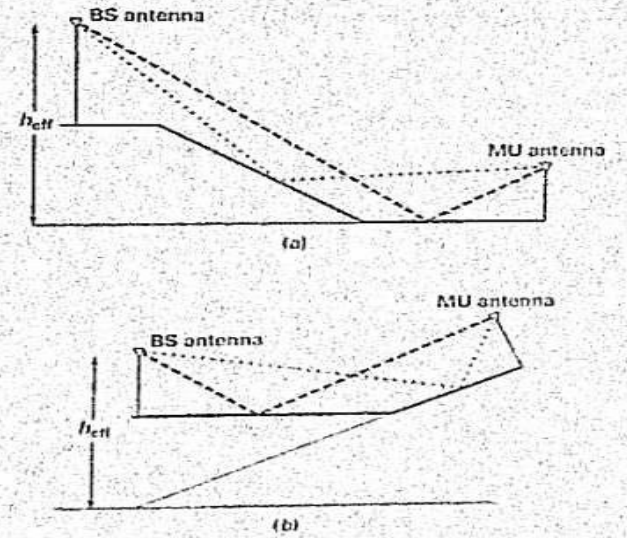

FIGURE 2.13 The concept of h_{eff}. (a) MU antenna on the ground. (b) MU antenna above the ground.

2.2 INDOOR PROPAGATION MODELS

The models discussed so far can be used to predict signal strength outdoors, but are not sufficient to predict signal strength indoors. Typical examples of indoor propagation are found in shopping malls, and in office buildings with different floors and room configurations. The variety of objects that reflect, scatter, and diffract the wireless signals include the different types of ceiling fixtures within a building, the different types of displays, and the different types of furniture. A model that can predict signal loss must take these different features into account (Bult 1987, 1989; Ders 1994; Molk 1991; Gane 1991). A building may have a very large room with no partitions and very few obstacles, or a very large room with a large number of obstacles. It is also possible for a building to have similar conditions in small rooms. The number of obstacles is not the only major factor in the determination of signal loss. The material used for partitioning the building also can adversely affect the strength of signal reaching the mobile user. This poses the challenge of coming up with a very general model that can predict the signal losses under all these conditions. The best approach for modeling propagation indoors is to classify these various environments into different "zone" configurations (Turk 1991b, Walk 1983, Samp 1997, Lots 1992, Rapp 1996b, Pars 1983). These configurations are based on the location of the base station and how the base station handles the traffic, and whether the base station is inside or outside the building.

2.2.1 Extra Large Zone

In an extra large zone there is a single base station outside the buildings that handles all the traffic in the buildings. This situation is ideal for a region that has a number of small offices or shops in adjoining buildings, as shown in Figure 2.14*a*.

Since the transmitting BS antenna is located outside the building, the signal will incur path-dependent losses as well as penetration-dependent losses because the signal must first traverse to the building boundary and then penetrate various floors and walls of the different buildings to reach the mobile unit. The median loss at a distance, d, from the transmitter in the extra large zone, $L_{ELZ}(d)$, can be expressed as

$$L_{ELZ}(d)\,(dB) = 10\log_{10}\left[L_f(d_0)\left(\frac{d}{d_0}\right)^{n_f} L_B(d_0)\left(\frac{d}{d_0}\right)^{n_B} A_B\right], \qquad (2.28)$$

where

$L_f(d_0)$ = attenuation due to propagation at $d = d_0$
$L_B(d_0)$ = attenuation due to building at $d = d_0$
n_f = attenuation factor of the propagation path loss with respect to distance
n_B = building attenuation factor
A_B = loss factor due to building penetration.

Note that quantities $L_f(d_0)$ and $L_B(d_0)$ are determined by the density of the obstacles present in the path as well as the frequency dependence of the losses. The distance-dependent loss parameter, n_f, is about 2 if there are very few obstacles (nearly free-space propagation), and if there are a lot of scattering centers n_f can be in the range of 3–6, as described in Section 2.1. The parameter n_B usually is in the range of 0.5–1.5. The quantity A_B depends on the difference between the heights of the transmitting and receiving antennas as well as on the materials in the building.

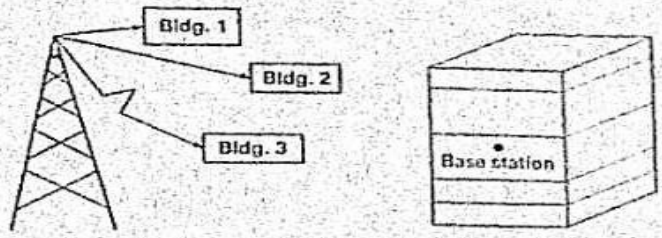

FIGURE 2.14 (a) Extra large zone. A single BS antenna is stationed outside the building. (b) Large zone. The base station is located in the building.

2.2.2 Large Zone

In a large zone, the building is very large but has a low population density. In this classification, a single base station is housed within the building itself. This situation is illustrated in Figure 2.14*b*.

The median loss in a large-zone system, $L_{LR}(d)$, can be expressed by simplifying eq. (2.28), for the loss in the extra large zone, as

$$L_{LR}(d)\,(\text{dB}) = 10\log_{10}\left[L_f(d_0)\left(\frac{d}{d_0}\right)^{n_f}\right], \qquad (2.29)$$

where n_f is the loss parameter. It will be in the range 2–3 if the transmitter and receiver are on the same floor, and it will be greater than 3 if they are on different floors.

2.2.3 Middle Zone

In the middle zone, the building structure is large and also heavily populated. This is a situation that commonly exists in shopping malls.

In this classification, a number of base stations are located within the building to serve the mobile phone users. A typical scenario for a single base station located within the building structure is shown in Figure 2.15. The median loss in the middle-zone system, $L_{MD}(d)$, can be expressed as

$$L_{MD}(d)\,(\text{dB}) = 10\log_{10}\left[\left(\frac{4\pi f_0 d}{c}\right)^2 F(d)^{k_1} W(d)^{k_2} R(d)\right], \qquad (2.30)$$

where

f_0 = carrier frequency
c = velocity of the electromagnetic wave
$F(d)$ = floor loss
$W(d)$ = wall loss
$R(d)$ = reflection loss
k_1 = number of floors in the path
k_2 = number of walls in the path

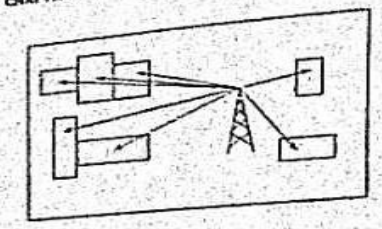

FIGURE 2.15 Middle zone. A base station is located within the structure to serve the MU in a portion of the structure. Similar base stations are present in other parts of the building.

2.2.4 Small Zone and Microzone

A building can have many partitions, with the penetration of the signal depending heavily on the material properties of the walls and partitions. This requires the provision of one base station for each room in the building. The loss models for the small zone can be obtained using the results for the large zone by incorporating the appropriate value of the loss parameter, r, based on the number and types of obstacles between the transmitter and receiver. If LOS conditions exist, r will be 2; for N-LOS conditions, r will be close to 3.5.

The conditions of the building may be such that there is heavy traffic within each room, and this will require the use of several base stations within a single room. Path loss calculations for the microzone can be done similarly to those for the small zone, using slightly smaller values of the loss parameter r.

2.3 FADING

As discussed earlier, the transmission characteristics are not determined by attenuation alone. The loss or attenuation observed may also fluctuate with distance and time, and this can be described in terms of fading.

When a signal leaves the transmitting antenna, it gets reflected, scattered, diffracted, or refracted by the various structures in its path (Arre 1973, Jake 1974, Gupt 1985, Fleu 1996, Hamm 1998, Stee 1999). We examined the signal loss arising from the presence of various obstacles in the channel. We also observed that the transmission loss fluctuates around a mean or median value. This aspect of the transmission loss curve, where the received signal loses its deterministic nature and becomes random in time and space, is described in terms of fading. In other words, fading is the process that describes the fluctuations in the received signal as the signal travels to the receiving antenna. Fading can be described either in terms of the primary cause (multipath or Doppler), the statistical distribution of the received envelope (Rayleigh, Rician, or lognormal), the duration of fading (long-term or short-term), or fast versus slow fading (Turi 1972, Stei 1987). We will look at these different characterizations of fading to understand their origin and specific consequences. We will also look at the various forms of fading to establish the relationships that exist among them.

2.3.1 Multipath Fading

Multipath fading, as the name suggests, arises from the existence of multiple paths between the transmitter and receiver. When a signal leaves the transmitting antenna, it can take a number of different paths to reach the receiver, as shown in Figure 2.16.

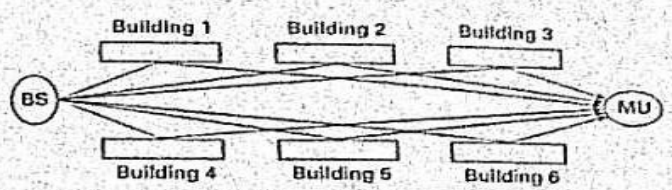

FIGURE 2.16 The multipath concept.

The mobile unit receives signal components that are scattered, reflected, diffracted, etc. by the buildings or by other artificial or natural structures, creating a number of different paths (Hodg 1990a, Ikeg 1980, Runm 1986, Brau 1991, Rapp 1996b).

We assume that the signal components scattered by these different structures arrive at the receiving antenna independently of each other, as shown in Figure 2.17. Under this condition, the signal received at the antenna can be expressed as the vector sum of the components coming from these structures.

For the time being, we also assume that the receiver is stationary. The received signal $e_r(t)$ can then be expressed as a sum of delayed components:

$$e_r(t) = \sum_{i=1}^{N} a_i p(t - t_i), \tag{2.31}$$

where a_i is the amplitude of the scattered component, $p(t)$ is the transmitted pulse shape, and t_i is the time taken by the pulse to reach the receiver. N is the number of different paths taken by the signal to reach the receiver. Note that we also make the assumption that no direct path exists between the transmitting and receiving antennae. Instead of writing the received signal amplitude as the sum of delayed components, we can also use phasor notation to represent the received signal:

$$e_r(t) = \sum_{i=1}^{N} a_i \cos(2\pi f_0 t + \phi_i), \tag{2.32}$$

where f_0 is the carrier frequency. The ith signal component has an amplitude of a_i and a phase of ϕ_i. The difference between eq. (2.31) and eq. (2.32) is the assumption of a single signal of carrier frequency f_0 in eq. (2.32) versus the transmission of a pulse in eq. (2.31). We will go back to eq. (2.31) later.

Equation (2.32) can be rewritten in terms of *in-phase* and *quadrature* notation as

$$e_r(t) = \cos(2\pi f_0 t) \sum_{i=1}^{N} a_i \cos(\phi_i) - \sin(2\pi f_0 t) \sum_{i=1}^{N} a_i \sin(\phi_i), \tag{2.33}$$

FIGURE 2.17 Conceptual "ray" diagram of the multipath between the transmitter and receiver.

where the first summation is identified as the *in-phase* term and the second summation is identified as the *quadrature* term.

If the locations of the structures are completely random, one can safely assume that the phase ϕ_i will be uniformly distributed (Papo 1991) in the range $(0, 2\pi)$. Under conditions of large N, the amplitude of the received signal can then be expressed as

$$c_r(t) = X\cos(2\pi f_0 t) - Y\sin(2\pi f_0 t), \tag{2.34a}$$

where

$$X = \sum_{i=1}^{N} a_i \cos(\phi_i), \quad Y = \sum_{i=1}^{N} a_i \sin(\phi_i). \tag{2.34b}$$

X and Y will be independent, identically distributed Gaussian random variables by virtue of the Central Limit Theorem (Papo 1991). Under these conditions, the envelope of the received signal, A, given by $(X^2 + Y^2)^{1/2}$, will be Rayleigh distributed. The envelope can be recovered through demodulation, which is discussed in Chapter 3. The probability density function $f_A(a)$ is given by

$$f_A(a) = \frac{a}{\sigma^2}\exp\left(-\frac{a^2}{2\sigma^2}\right)U(a), \tag{2.35}$$

where the parameter σ^2 is the variance of the random variable X (or Y) and $U(.)$ is the unit step function. Note that if the envelope of the signal is Rayleigh distributed, the power, P, will have an exponential distribution, given by

$$f_P(p) = \frac{1}{2\sigma^2}\exp\left(-\frac{p}{2\sigma^2}\right)U(p). \tag{2.36}$$

The Rayleigh and exponential probability density functions are shown in Figure 2.18. The Rayleigh-distributed envelope is characterized by a mean given by

$$E(A) = \sigma_A\sqrt{\frac{\pi}{2}} \tag{2.37}$$

and a variance, σ_A^2, given by

$$\sigma_A^2 = \sigma^2\left[2 - \frac{\pi}{2}\right]. \tag{2.38}$$

Note that the Rayleigh distribution is also unique in terms of its ratio of the mean to the standard deviation:

$$\frac{E(A)}{\sigma_A} = 1.91. \tag{2.39}$$

Plots of the radio-frequency (rf) signal and the corresponding envelope under Rayleigh fading are shown in Figure 2.19. We see that the received signal power is random even in the absence of noise introduced by the electronic system, namely, the additive white Gaussian noise. This is a consequence of the existence of multiple paths and the randomness of the phase (Auli 1979). Multipath fading thus leads to fluctuations in the received signal when the MU moves from place to place.

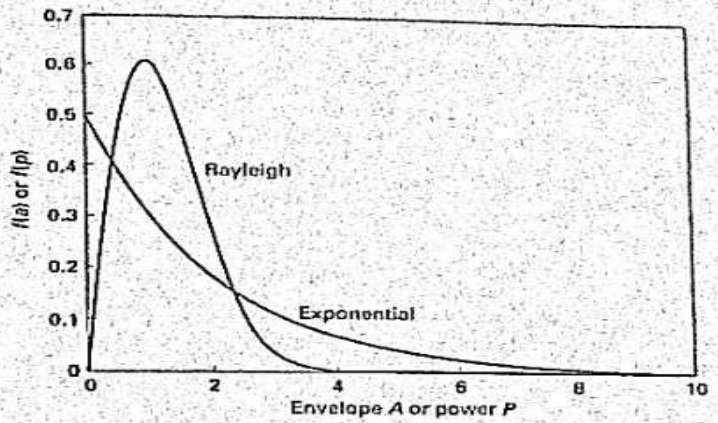

FIGURE 2.18 The density functions of the Rayleigh-distributed envelope and exponentially distributed power.

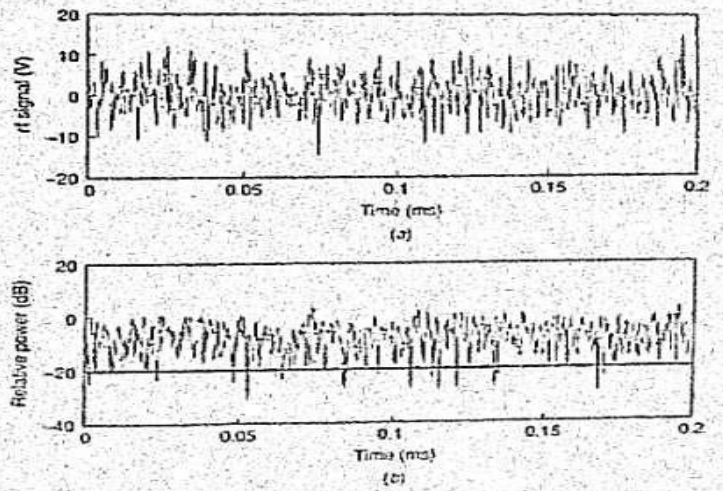

FIGURE 2.19 Rayleigh-faded rf signal (a) and its power (b). The plots were generated from 11 multiple paths. The envelope was obtained by demodulating the rf signal.

Note that we have not taken into account the fact that the MU may be moving at a certain speed.

To understand the implications of this fluctuation in the received power, consider the following scenario. If the receiver is designed to operate at an acceptable level only if a certain minimum power, P_{thr}, is being received, the receiver goes into outage whenever the power goes below this threshold value (Jake 1974, Ikegage 1980, Pale 1991). In Figure 2.19, we can clearly see that the system goes into outage if the threshold is set to −20 dB of relative power (indicated by the line drawn parallel to the frequency axis in Figure 2.19b). The *outage probability*, P_{out}, can now be calculated as

$$P_{out} = \int_0^{P_{thr}} f(p)\,dp = \int_0^{P_{thr}} \frac{1}{P_0}\exp\left(-\frac{p}{P_0}\right)dp = 1-\exp\left(-\frac{p}{P_0}\right). \qquad (2.40)$$

where P_0 is the average power, given by $2\sigma^2$. One of the adverse consequences of fading is the existence of outage. When outage occurs, the performance of the wireless system becomes unacceptable.

EXAMPLE 2.4

Consider the case of a Rayleigh-fading channel. If the average power being received is 100 μW, what is the probability that the received power will be less than 50 μW?

Answer Using eq. (2.40), the probability is $[1-\exp(-50/100)] = 0.3935$. □

EXAMPLE 2.5

If the minimum required power for acceptable performance is 25 μW, what is the outage probability in a Rayleigh channel with an average received power of 100 μW?

Answer Using eq. (2.40), the probability of outage is $[1-\exp(-25/100)] = 0.2212$, or 22.1%. □

2.3.2 Dispersive Characteristics of the Channel

The fluctuation of the received power is not the only effect of fading. Fading may also affect the shape of the pulse as it is being transmitted through the channel (Cox 1972, 1975; Hash 1979, 1989). Consider the diagram of multipath fading shown in Figure 2.20, corresponding to eq. (2.31). Only four different paths are shown. Because of the different paths taken, the replicas of the pulse will arrive at the receiver at four different times. If these pulses are not resolvable, the effect of the multipath is to produce a broadened pulse, as shown by the envelope of the overlapping pulses. In other words, the multipath effect can result in broadening of the transmitted pulse, leading to intersymbol interference (ISI) (see Section B.6, Appendix B).

The situation shown in Figure 2.20 can be simulated using MATLAB. The results are shown in Figure 2.21. A Gaussian pulse of width $\sigma_d = 14.14$ ms is being transmitted through a wireless channel. Ten different paths have been selected to replicate the scenario described in the previous paragraph. These pulses have different time delays, randomly chosen and having random power as they reach the receiver. A

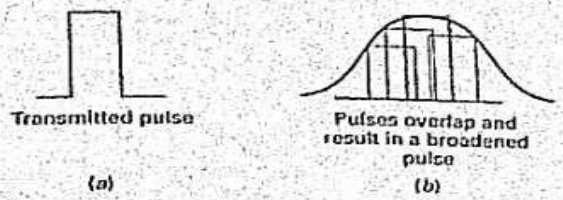

FIGURE 2.20 (a) A transmitted pulse. (b) The multiple pulses produced due to the multipath arriving at different times and with different powers, leading to a broadened envelope of the pulse.

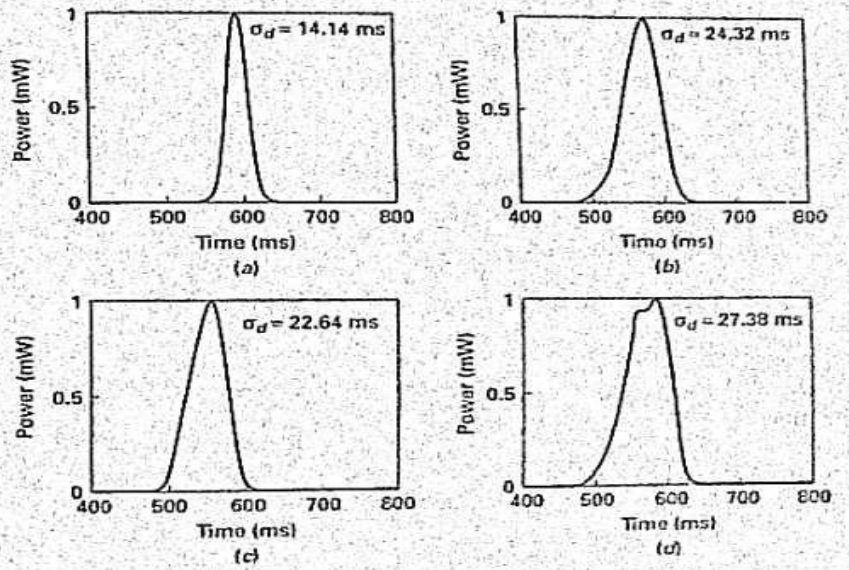

FIGURE 2.21 The frequency-selective fading channel simulated using MATLAB.

single pulse corresponding to one of the paths is shown in Figure 2.21*a*; this pulse is simply a delayed version of the transmitted pulse. In the absence of multiple paths, the pulse width remains the same as that of the transmitted pulse. Figures 2.21*b*, *c*, and *d* show the received pulse (the sum of the 10 multipath components) for three different simulations. The power has been normalized to unity. The standard deviation of each pulse is also indicated. It is obvious that the pulses have broadened. This is demonstrated by the increase in the pulse width of the received pulse compared with the transmitted pulse (Figure 2.21*a*). The situation depicted in Figure 2.20*b* is shown in Figures 2.21*b*, *c*, and *d*.

This dispersive behavior of the channel can be qualitatively described in the following manner. (The reasons for referring to this behavior of the channel as dispersive will be clear later.) Consider the transmission of a very narrow pulse

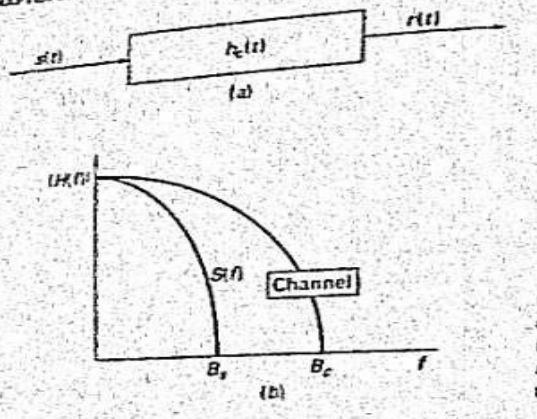

FIGURE 2.24 The baseband channel response (transfer function) of a "flat" channel along with the spectrum of the transmitted signal $S(f)$.

subjected to dispersive behavior, resulting in pulse broadening, and consequently the components will experience ISI (see Figure 2.25). The channel is thus classified as a *frequency-selective* channel (Bell 1963a, Jake 1974). The impulse response shown in Figure 2.22*b* can be viewed as an example of a frequency-selective channel. Note, however, that the distinction between flat and frequency-selective channels must be based on the relationship between the information bandwidth and σ_τ, and not on the absolute value of σ_τ. Thus, a flat channel becomes a frequency-selective one if the information is transmitted at a higher and higher data rate. We can now understand why we refer to a frequency-selective channel as a dispersive channel. The frequency-selective channel behaves as if different frequency components travel at different speeds (phenomenon of dispersion) and arrive at different times at the receiver, leading to pulse broadening.

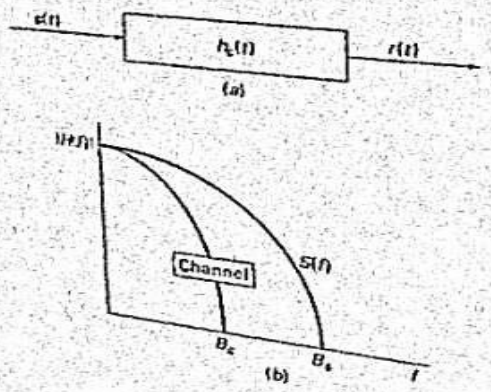

FIGURE 2.25 The baseband channel response (transfer function) of a "frequency-selective" channel (*a*) along with the spectrum of the transmitted signal (*b*), $S(f)$.

EXAMPLE 2.6

A typical impulse response of a wireless channel is given in Figure E2.6. If the data rate is 240 kbps, classify the channel as frequency-selective or flat.

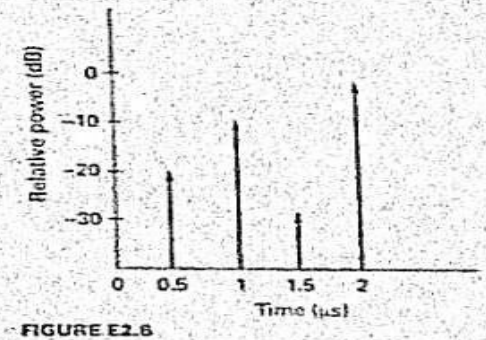

FIGURE E2.6

Answer $P(0.5) = 0.01$, $P(1) = 0.1$, $P(1.5) = 0.001$, and $P(2) = 1$, with $\sum_i P_i = 1.111$.

$$\langle \tau \rangle = \frac{0.5 \times 0.01 + 1 \times 0.1 + 1.5 \times 0.001 + 2 \times 1}{1.111} = 1.595\ \mu s$$

$$\langle \tau^2 \rangle = \frac{0.25 \times 0.01 + 1 \times 0.1 + 2.25 \times 0.001 + 4 \times 1}{1.111} = 3.695\ \mu s^2$$

$$\sigma_\tau = \sqrt{3.695 - 1.595^2} = 0.315\ \mu s$$

$B_c = 675$ kHz > 240 kHz. The channel is therefore "flat." □

We see that the two effects, the randomness of the received signal envelope and the frequency selectivity of the channel, are separate manifestations of the multipath propagation and can exist alone or in combination. However, in most practical cases, the received signal phases are random, and the Rayleigh distribution of the envelope will be exhibited irrespective of the frequency-selective nature of the channel.

One of the best ways to describe the frequency-dependent behavior of the channel is to use a two-ray model to represent the fading. In this model (Walk 1966, Clar 1968, Hash 1979, Ball 1982, Casa 1990), the impulse response, $h_c(t)$, of the channel is written as the sum of two Rayleigh fields having random phases and a delay of τ:

$$h_c(t) = a_1 \exp(j\phi_1)\delta(t) + a_2 \exp(j\phi_2)\delta(t - \tau). \tag{2.45}$$

where a_1 and a_2 are independent, identically distributed Rayleigh variables, and ϕ_1 and ϕ_2 are uniformly distributed in the range $(0, 2\pi)$. If a_2 is zero, we have a flat fading channel. By varying τ, it is possible to create channels with different bandwidths. Consider a simple case where a_1 and a_2 are scalars and deterministic with $b = a_2/a_1$. Assuming ϕ_1 and ϕ_2 to be deterministic and equal, eq. (2.45) for the impulse response can be rewritten as

$$h_c(t) = \delta(t) + b\delta(t - \tau). \tag{2.46}$$

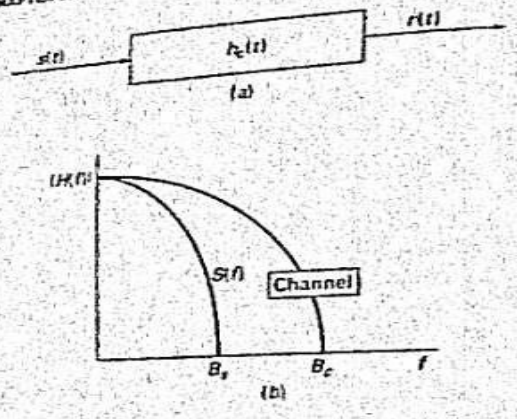

FIGURE 2.24 The baseband channel response (transfer function) of a "flat" channel along with the spectrum of the transmitted signal $S(f)$.

subjected to dispersive behavior, resulting in pulse broadening, and consequently the components will experience ISI (see Figure 2.25). The channel is thus classified as a *frequency-selective* channel (Bell 1963a, Jake 1974). The impulse response shown in Figure 2.22b can be viewed as an example of a frequency-selective channel. Note, however, that the distinction between flat and frequency-selective channels must be based on the relationship between the information bandwidth and σ_d, and not on the absolute value of σ_d. Thus, a flat channel becomes a frequency-selective one if the information is transmitted at a higher and higher data rate. We can now understand why we refer to a frequency-selective channel as a dispersive channel. The frequency-selective channel behaves as if different frequency components travel at different speeds (phenomenon of dispersion) and arrive at different times at the receiver, leading to pulse broadening.

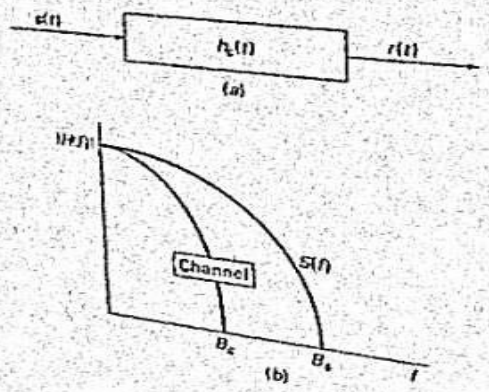

FIGURE 2.26 The baseband channel response (transfer function) of a "frequency-selective" channel (a) along with the spectrum of the transmitted signal (b), $S(f)$.

EXAMPLE 2.6

A typical impulse response of a wireless channel is given in Figure E2.6. If the data rate is 240 kbps, classify the channel as frequency-selective or flat.

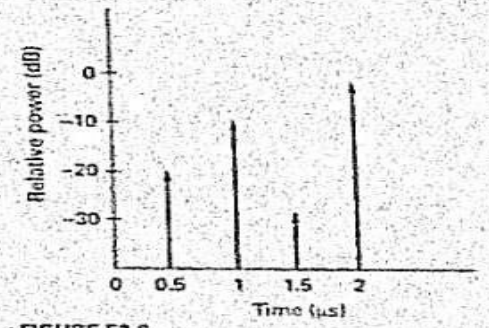

FIGURE E2.6

Answer $P(0.5) = 0.01$, $P(1) = 0.1$, $P(1.5) = 0.001$, and $P(2) = 1$, with $\sum_i P_i = 1.111$.

$$\langle \tau \rangle = \frac{0.5 \times 0.01 + 1 \times 0.1 + 1.5 \times 0.001 + 2 \times 1}{1.111} = 1.595\ \mu s$$

$$\langle \tau^2 \rangle = \frac{0.25 \times 0.01 + 1 \times 0.1 + 2.25 \times 0.001 + 4 \times 1}{1.111} = 3.695\ \mu s^2$$

$$\sigma_d = \sqrt{3.695 - 1.595^2} = 0.315\ \mu s$$

$B_s = 675$ kHz > 240 kHz. The channel is therefore "flat." □

We see that the two effects, the randomness of the received signal envelope and the frequency selectivity of the channel, are separate manifestations of the multipath propagation and can exist alone or in combination. However, in most practical cases, the received signal phases are random, and the Rayleigh distribution of the envelope will be exhibited irrespective of the frequency-selective nature of the channel.

One of the best ways to describe the frequency-dependent behavior of the channel is to use a two-ray model to represent the fading. In this model (Walk 1966, Clar 1968, Hash 1979, Ball 1982, Cassa 1980), the impulse response, $h_c(t)$, of the channel is written as the sum of two Rayleigh fields having random phases and a delay of τ:

$$h_c(t) = a_1 \exp(j\phi_1)\delta(t) + a_2 \exp(j\phi_2)\delta(t - \tau). \tag{2.45}$$

where a_1 and a_2 are independent, identically distributed Rayleigh variables, and ϕ_1 and ϕ_2 are uniformly distributed in the range $(0, 2\pi)$. If a_2 is zero, we have a flat fading channel. By varying τ, it is possible to create channels with different bandwidths. Consider a simple case where a_1 and a_2 are scalars and deterministic with $b = a_2/a_1$. Assuming ϕ_1 and ϕ_2 to be deterministic and equal, eq. (2.45) for the impulse response can be rewritten as

$$h_c(t) = \delta(t) + b\delta(t - \tau). \tag{2.46}$$

and the corresponding transfer function, $H_c(f)$, of the frequency-selective channel will be given by

$$H_c(f) = 1 + b\exp(-j2\pi f\tau). \tag{2.47}$$

The behavior of a typical channel may be observed by plotting the absolute value of the transfer function:

$$|H_c(f)| = \sqrt{1 + b^2 + 2b\cos(2\pi f\tau)}. \tag{2.48}$$

A plot of $|H_c(f)|$ is shown in Figure 2.26.

The transfer function has "notches" at intervals of $f\tau = 1$. For different values of τ, the bandwidth of the channel measured by the zero crossing will vary, causing the channel to go from being flat to being frequency selective. Note that in this simple description we have assumed the scaling factors to be deterministic. In practice, the scaling factors are random (Rayleigh distributed).

2.3.3 Time-Dispersive Behavior of the Channel

So far we have considered only the case of a stationary mobile unit. Consider now the case of a mobile unit traveling at speed v, as shown in Figure 2.27. The motion of the mobile unit will result in a Doppler shift in the frequency of the signal being received. The maximum Doppler shift, f_d, can be expressed as

$$f_d = f_0\frac{v}{c}, \tag{2.49}$$

where c is the velocity of the electromagnetic wave in free space. Taking all possible directions into account, the instantaneous frequency, f_{in}, will be given by

$$f_{in} = f_0 + f_d\cos(\theta_i). \tag{2.50}$$

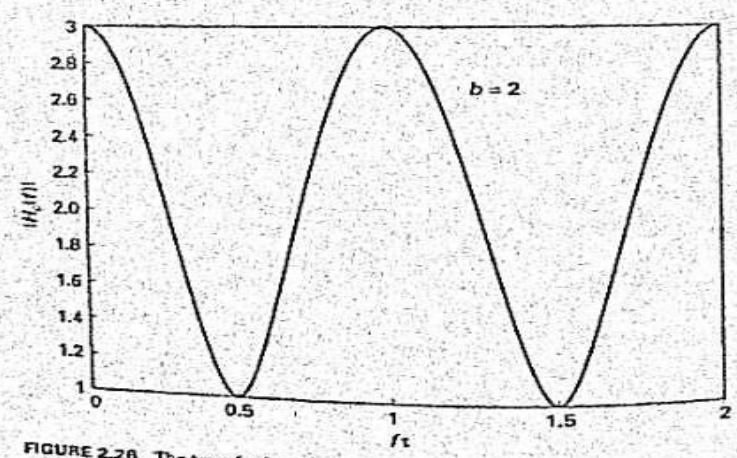

FIGURE 2.26 The transfer function of a "two-ray" model to describe the frequency-selective channel.

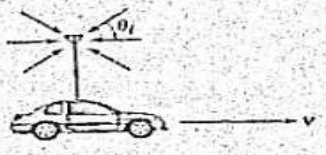

FIGURE 2.27 A mobile unit moving at speed v.

The received signal can once again be expressed as

$$c_r(t) = \cos(2\pi f_0 t)\sum_{i=1}^{N} a_i\cos[2\pi f_d\cos(\theta_i)t + \psi_i] - \sin(2\pi f_0 t)\sum_{i=1}^{N} a_i\sin[2\pi f_d\cos(\theta_i)t + \psi_i], \tag{2.51}$$

where N is the number of multipaths available and ψ_i are the phases. If we make the assumption that N is sufficiently large, the envelope will be Rayleigh distributed as in the case of the stationary MU. A typical plot of the Doppler-faded signal is shown in Figure 2.28.

We can also calculate the power spectrum of the received signal (Gans 1972, Huan 1992, Pars 1992, Fleu 1996, Stee 1999). Equation (2.50) shows that the received signal will have a carrier frequency shifted by an amount $\pm f_d\cos(\theta_i)$. For a MU moving in a street, θ_i can be either zero or π, and the extreme values of the Doppler shift

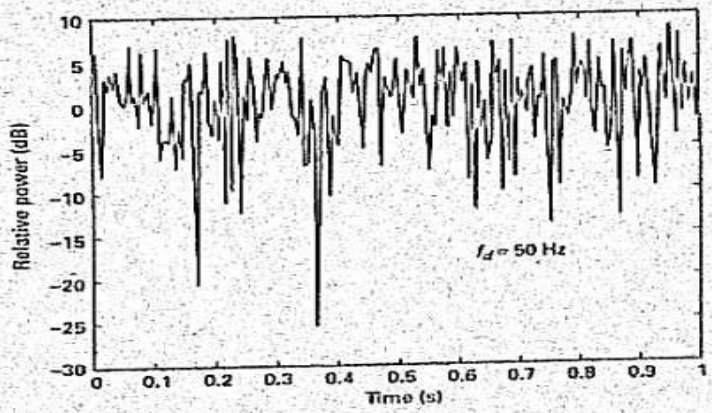

FIGURE 2.28 A Doppler-faded signal.

will be $\pm f_d$. If we make the assumption that the phases, ψ_i, and θ_i are uniform in the range $(0, 2\pi)$, the power spectrum, $S_d(f)$, of the received signal $c_r(t)$ can be expressed as (Gans 1972, Jake 1974)

$$S_d(f) = \begin{cases} \dfrac{\sigma^2}{\pi f_d \sqrt{1-\left(\dfrac{f}{f_d}\right)^2}} & |f| \le f_d \\ 0 & \text{otherwise.} \end{cases} \tag{2.52}$$

A plot of the power spectrum is shown in Figure 2.29. It shows that most of the energy is concentrated around the maximum Doppler shift, f_d. Note that the power spectrum depends on the radiation pattern of the antenna and the polarization used.

Consider now the transmission of a short rf pulse as the vehicle is in motion. The motion of the MU will now introduce changes in the channel at a rate of f_d Hz. If the duration of the pulse is very short, the changes introduced by the motion will be very slow and will have very little or no impact on the transmission and, therefore, on the reception of the pulse. In other words, if the bandwidth of the signal measured in terms of the inverse of the pulse duration is much larger than the maximum Doppler shift, the channel will vary very slowly or will be a slow-fading channel. On the other hand, if the duration of the pulse is large, changes introduced in the channel from the motion of the mobile unit will be "fast" and thus will affect the transmission. In other words, for transmission at a very low data rate, a moving vehicle will introduce fast fading if the bandwidth of the signal is not much larger than the maximum Doppler shift.

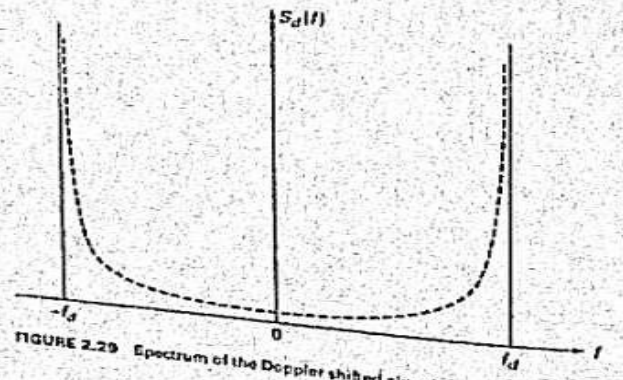

FIGURE 2.29 Spectrum of the Doppler shifted signal.

The condition for slow versus fast fading can now be expressed in terms of the coherence time, T_c, of the channel (Stei 1987), measured in terms of the inverse of the maximum Doppler shift given by (see Section C.1, Appendix C)

$$T_c = \frac{9}{16\pi f_d}. \tag{2.53}$$

If the pulse duration is smaller than T_c, the pulses are unlikely to undergo distortion (slow fading), and if the pulse duration is larger than the coherence time, the pulses undergo fast fading and will be distorted. Fast fading is thus a frequency-dispersive property of the channel brought on by the motion of the mobile unit. The difference between distortion and dispersion is explained in Appendix C.

EXAMPLE 2.7

Consider an antenna transmitting at 900 MHz. The receiver, a MU, is traveling at a speed of 30 km/h and is receiving/transmitting data at 200 kbps. Examine whether the channel fading is slow or fast.

Answer The Doppler shift is given by

$$f_d = \frac{9\times10^8 \times 30 \times 1000}{3600 \times 3 \times 10^8} = 25 \text{ Hz}.$$

The coherence time is

$$T_c = \frac{9}{400\pi} = 7162\,\mu\text{s} \gg \frac{1}{200\times10^3}.$$

The channel is therefore a "slow-fading" one. □

2.3.4 Level Crossing and Average Fade Duration

One of the important consequences of Doppler fading is that the signal will experience deep fades occasionally as the vehicle is in motion (Lee 1967, Kenn 1969, Bodt 1982, Adac 1988b, Pars 1992). The analysis of fading in terms of Rayleigh statistics does not allow a clear understanding of how often deep fades occur or how long they last; Rayleigh statistics merely provide information on the overall percentage of time that the signal goes below a certain level. Information is needed on the rate at which deep fades occur and their duration, so that system designers can choose specific approaches for appropriate data rates, word lengths, and coding schemes to mitigate the effects of deep fades.

Deep fades can be quantitatively expressed using the parameters level crossing rate, N_A, and average fade duration, τ_A. To understand the concept of level crossing, consider the envelope of a signal received from a moving vehicle as shown in Figure 2.30. The envelope of the signal is seen to fluctuate in time. The level crossing rate is defined as the expected rate at which the envelope crosses a specified signal level A in the positive direction, as shown in Figure 2.30, and is given by

$$N_A = \int_0^\infty \dot{a} p(A, \dot{a}) d\dot{a}, \tag{2.54}$$

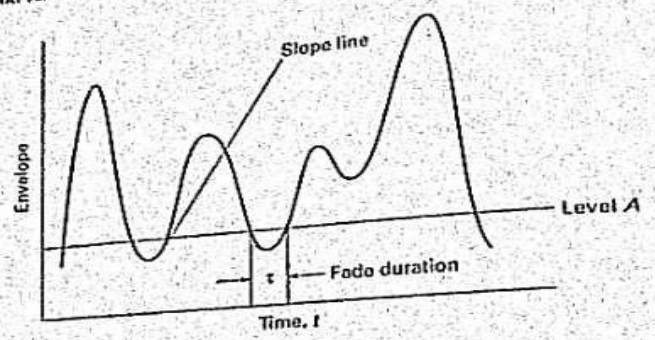

FIGURE 2.30 The concept of level crossing.

where $\dot{a}$ is the derivative of $a(t)$ and $p(A, \dot{a})$ is the joint probability density function of the level A and the rate of change of $a(t)$. Based on the results of Rice (Lee 1967, Kenn 1969), the expression for the level crossing rate, N_A, becomes

$$N_A = \sqrt{2\pi} f_d \alpha e^{-\alpha^2}, \tag{2.55}$$

where α is the ratio A/A_{rms}. (A_{rms} is the rms value of the envelope.) The level crossing rate also depends on the maximum Doppler shift, f_d, and therefore on the speed of the mobile unit. By virtue of the factor $\alpha e^{-\alpha^2}$, there will be fewer crossings at low values of the signal level as well as at high values of the signal level. Certainly there will be more level crossings at higher speeds of the mobile unit.

Another parameter of interest is the average fade duration, τ_{av}, which is the average period of time the signal stays below a certain level A. For the case of Rayleigh fading, the average fade duration is given by

$$\tau_{av} = \frac{1}{N_A} \text{prob}(a \le A), \tag{2.56}$$

where $\text{prob}(a \le A)$, the probability that the instantaneous signal is less than A, is given by

$$\text{prob}(a \le A) = 1 - e^{-\alpha^2}. \tag{2.57}$$

Using eqs. (2.56) and (2.57), the average fade duration τ_{av} is given as

$$\tau_{av} = \frac{e^{\alpha^2} - 1}{\sqrt{2\pi}\alpha f_d}. \tag{2.58}$$

These two parameters are useful in enabling assessment of the instantaneous bit error rates, since the overall performance is determined not only by the error probabilities on a long-range basis but also by how the error rates vary on a short-term basis. The presence of deep fades as well as the number of such fades will change the instantaneous signal-to-noise ratio and hence, the bit error rates.

EXAMPLE 2.8

Continuing Example 2.7, calculate the average fade duration if $\alpha = 0.1$.

Answer

$$\text{Doppler shift} = 25 \text{ Hz}$$

$$\tau_{av} = \frac{e^{\alpha^2} - 1}{\sqrt{2\pi}\alpha f_d} = 1600 \,\mu\text{s}$$

□

2.3.5 Frequency Dispersion versus Time Dispersion

We have seen that fading can occur in the frequency domain or in the time domain. It is possible to treat fading in wireless communications systems as constituted by independent effects. The channel shows frequency-dispersive behavior when multipath phenomena are present. At the same time, the channel exhibits time dispersion if the mobile unit is moving. Even though these are independent effects, a relationship exists between these two dispersive attributes of the channel due to the uncertainty principle relating time and frequency dependence. This effect is demonstrated in Figure 2.31.

At very low data rates, the pulse duration is high and the channel is primarily slow and flat. If the data rate is very high and the MU is moving slowly, the channel will be slow but frequency selective. If, however, the data rate is high and the MU is moving at a very high speed, the channel will be fast and frequency selective. Channels falling in this category suffer from both time dispersion and frequency dispersion, and require additional corrective measures to overcome the distortion.

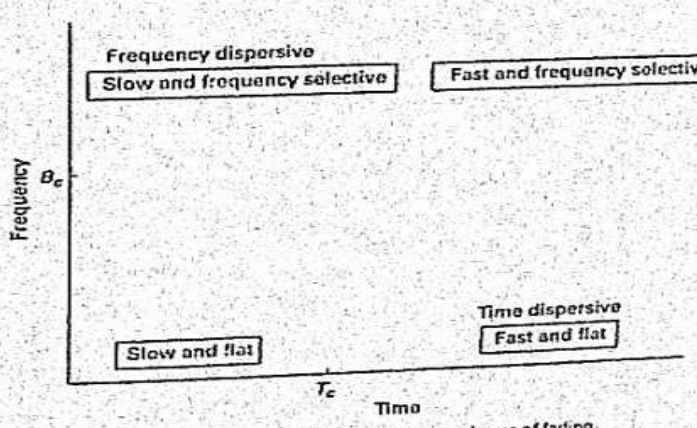

FIGURE 2.31 The "regions" of influence of different forms of fading.

2.4 OTHER FADING MODELS

2.4.1 Rician Fading

Rayleigh fading is not the only consequence of the multipath phenomenon (Stel 1964, Hash 1993). In addition to a number of random paths taken by the signal, it is possible to have a line-of-sight (LOS) propagation from the transmitter to the receiver. This LOS signal adds a deterministic component to the multipath signal. This is shown in Figure 2.32 and is compared with the case of Rayleigh fading.

The deterministic component makes the Gaussian random variable (eq. 2.32) one of nonzero mean, and consequently the envelope is Rician distributed. The pdf of the envelope can be expressed as (Papo 1991, Dave 1958)

$$f_A(a) = \frac{a}{\sigma^2}\exp\left(-\frac{a^2+A_0^2}{2\sigma^2}\right)I_0\left(\frac{aA_0}{\sigma^2}\right), \tag{2.59}$$

where $I_0(.)$ is the modified Bessel function and A_0 is the component arising from the LOS signal. In the literature, it is customary to refer to the contribution of the randomly located scattering centers as the "diffuse" component and the contribution of the LOS component as the "steady" component. We therefore say that Rayleigh fading is the result of diffuse components and Rician fading is the result of the presence of a steady component along with the diffuse components.

The Rician probability density function is often characterized by the ratio of the power of the direct component to the power of the diffuse component, K (dB):

$$K(\text{dB}) = 10\log_{10}\left(\frac{A_0^2}{2\sigma^2}\right). \tag{2.60}$$

For $K = -\infty$, we have no direct path and the Rician distribution becomes Rayleigh. For higher and higher values of K, the Rician distribution becomes almost Gaussian.

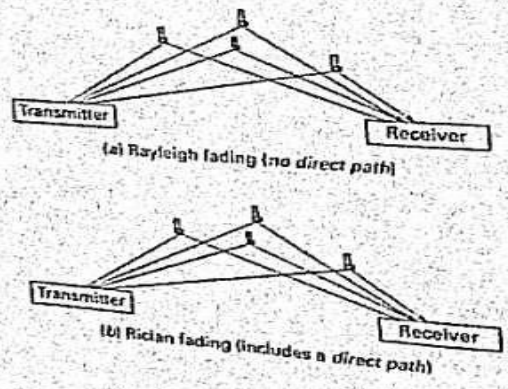

FIGURE 2.32 Comparison of the conditions that exist for (a) Rayleigh fading and (b) Rician fading.

The Rician probability density function is shown in Figure 2.27 for different values of the parameter K.

The transition from Rayleigh to Gaussian can be seen clearly in Figure 2.33 as the value of K continues to increase. The LOS component of the Rician distribution provides a steady signal and serves to reduce the effects of fading.

EXAMPLE 2.9

In a wireless channel there is one direct path and six diffuse paths. The direct path has a power of 200% compared with the average power of any one of the diffuse paths. Find the Rician factor K.

Answer Note that in eq. (2.60) the denominator is the sum of the contributions of the average powers of the diffuse paths. Therefore, $K = 2/6$, or $10\log(2/6) = -4.7$ dB. ◻

2.4.2 Lognormal Fading

The fading described so far falls under the category of "short-term" fading. However, as shown in Figure 2.5, the received signal also undergoes "long-term" fading. Consider the geometry of the scattering shown in Figure 2.34, where the propagation takes place in an environment with tall structures (trees, buildings).

Under these conditions, the signal reaching the receiver will not be the result of a single scattering effect; it will be the result of multiple scattering (Suzu 1977, Lee 1985, Hans 1977, Fren 1979). For example, the signal is likely to be multiply reflected or scattered before taking multiple paths to the receiver. The signal received, $r(t)$, by the MU or the base station receiver can now be expressed as

$$r(t) = \sum_{n=1}^{N} a_n \exp(-j\phi_n t). \tag{2.61}$$

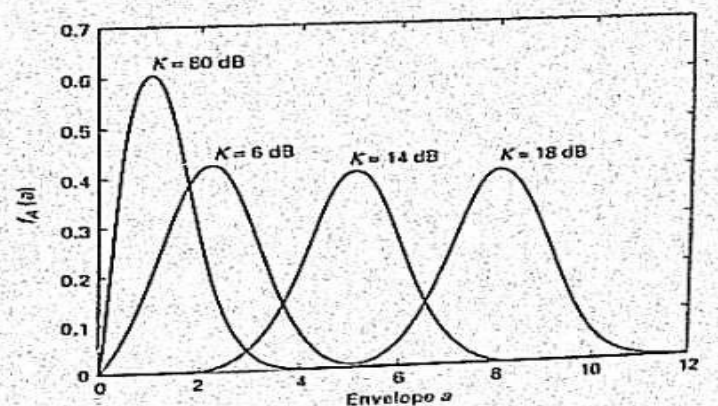

FIGURE 2.33 The Rician distribution for different values of K (dB).

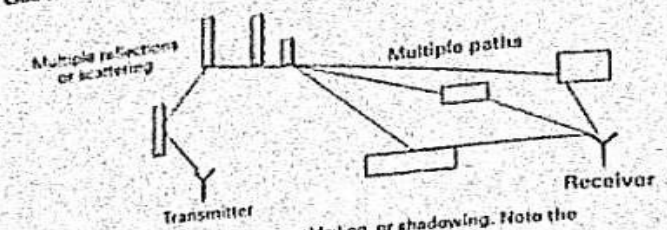

FIGURE 2.34 Geometry for lognormal fading, or shadowing. Note the existence of multiple reflections.

where the strengths of the multipath components are expressed as

$$a_n = \prod_{m=1}^{M} b_{mn}. \tag{2.62}$$

The quantities b_{mn} represent the scattering strengths of the multiply reflected components. Considering the fact that the region where the scattering takes place has a number of individual scatterers, the b_{mn} can be easily modeled as Rayleigh-distributed random variables. The impact of multiple scattering is to introduce further fluctuations in the received power, which will be manifested in the mean value of the received power, itself becoming random.

The mean value of the received power will be proportional to the variance of the Rayleigh-distributed envelope. However, the variance of the Rayleigh envelope will depend on $(b_{mn})^2$. The average signal power, P_{LT}, can then be expressed as

$$P_{LT} = \prod_{m=1} p_m, \tag{2.63}$$

where

$$p_m = b_{mn}^2. \tag{2.64}$$

Applying the Central Limit Theorem for the product of random variables (Papoulis 1991), the density function $f(p_{dB})$ of P_{dB}, the logarithm of P_{LT}, given by

$$P_{dB} = 10\log_{10}(P_{LT}) = \sum_{n=1} 10\log_{10}(p_n), \tag{2.65}$$

will be Gaussian and given by

$$f(p_{dB}) = \frac{1}{\sqrt{2\pi}\sigma_{dB}} \exp\left[-\frac{(p_{dB} - P_{av})^2}{2\sigma_{dB}^2}\right]. \tag{2.66}$$

The parameters appearing in this equation are

P_{av} = average power (dBm)

σ_{dB} = standard deviation (dB)

The pdf of the signal power P_{LT} under lognormal fading can now be expressed as

$$f(P_{LT}) = \frac{1}{\sqrt{2\pi\sigma^2}P_{LT}} \exp\left[-\frac{1}{2\sigma^2}\ln^2\left(\frac{P_{LT}}{P_0}\right)\right], \tag{2.67}$$

where p_0 is the average power in milliwatts and

$$\sigma = \frac{\sigma_{dB}\ln(10)}{10}. \tag{2.68}$$

Equation (2.67) is the lognormal pdf, and the multiple scattering leads to a lognormal distribution for the power received. The logarithm with respect to the base e is represented by ln. The lognormal pdf is shown in Figure 2.35. Lognormal fading is also referred to as *shadowing*, due to the fact that the shadowing seen in images can be modeled using an exponential transformation similar to the one given in eq. (2.63).

EXAMPLE 2.10

If the power received at the MU is lognormal with a standard deviation of 8 dB, calculate the outage probability. Assume that the average power being received is −95 dBm and the threshold power is −98 dBm. (Hint: Use the *erf* function. See Section B.7, Appendix B.)

Answer

$$P_{out} = \int_{-\infty}^{-98} \frac{1}{\sqrt{2\pi}\times 8} \exp - \frac{[x-(-95)]^2}{2\times 8^2} dx = 0.5 + 0.5\times \text{erf}\left[\frac{-98+95}{8\sqrt{2}}\right] = 0.3538$$

■

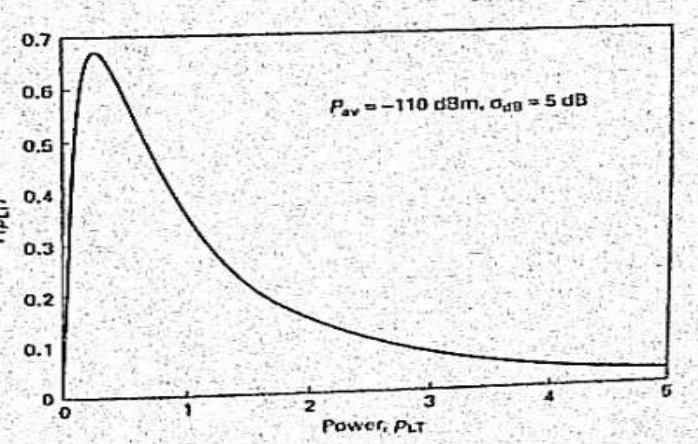

FIGURE 2.35 The lognormal probability density function.

fluctuation of the received power from lognormal fading creates additional problems for designers of the wireless link. Including lognormal fading, the expression for the received power in any general area can be expressed by modifying eq. (2.9) as follows:

$$P_r(d)\,\text{dBm} = 10\log_{10}[P_r(d_{ref})] + 10\nu\log_{10}\left[\frac{d_{ref}}{d}\right] + Y_\sigma, \qquad (2.69)$$

where Y_σ is a zero-mean random variable with a standard deviation of σ_{dB}. In other words, the received power in dBm will be Gaussian distributed, with the median value of the received power (dBm) being the average and σ_{dB} being the standard deviation. A typical curve for the case $\nu = 3$ and standard deviation of lognormal fading of 6 dB is shown in Figure 2.36. It is possible to see that at any given location, the received power could be less than the median value of the power estimated from the Hata model or any other model. This necessitates the establishment of a power margin to account for fading at least as much as the standard deviation of fading, which reduces the maximum transmission distance as indicated in the figure.

We will reexamine the effects of lognormal fading on the coverage area in Chapter 4.

2.4.3 Nakagami Distribution

The Rayleigh and Rician models of fading assume that the amplitudes of the scattered components from the different paths are equal. The Nakagami model is very general and allows for the possibility of different strengths for the scattered components (Hash 1993, Braa 1991, Heff 1960, Beck 1962). It can also work under conditions

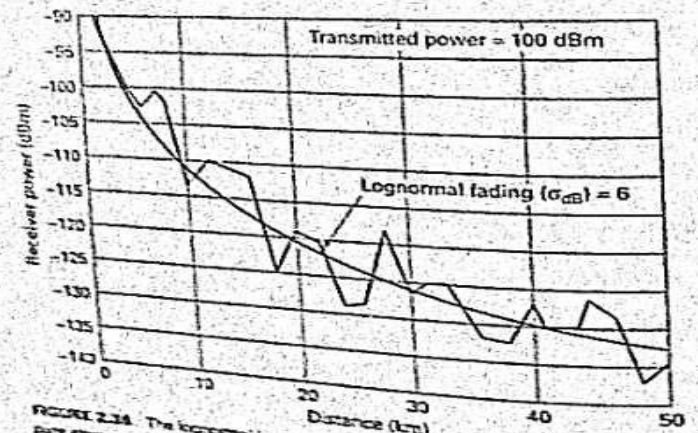

FIGURE 2.36 The lognormal long-term behavior (discontinuous line) versus path distance. Compare this with Figure 2.5.

where the possibility of partial correlation exists between scattering elements. The density function of the envelope can be expressed as

$$f_A(a) = \frac{2m^m a^{2m-1}}{\Gamma(m)\Omega^m}\exp\left(-\frac{ma^2}{\Omega}\right)U(a), \qquad (2.70)$$

where $\Gamma(\cdot)$ is the gamma function,

$$\Omega = \langle A^2 \rangle, \qquad (2.71)$$

and

$$m = \frac{\langle A^2 \rangle^2}{\langle (A^2 - \Omega)^2 \rangle}. \qquad (2.72)$$

There is an important restriction on the Nakagami parameter, that $m \geq 1/2$. For a value of $m = 1/2$, the Nakagami distribution becomes a single-sided Gaussian distribution. The Nakagami distribution becomes Rayleigh for $m = 1$, and for values of $m > 1$ the Nakagami distribution becomes Rician. The Nakagami probability density function is thus general enough to encompass both the Rayleigh and Rician distributions. The Nakagami probability density function is shown in Figure 2.37.

2.4.4 Suzuki Distribution

Rayleigh and lognormal fading have been considered to be two separate effects. However, the phenomena responsible for short-term fading (Rayleigh) and long-term fading (lognormal) occur concurrently (Suzu 1977, Fren 1979). The mean

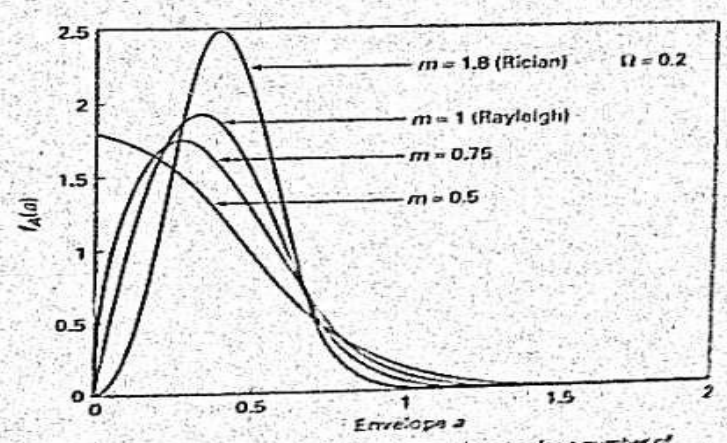

FIGURE 2.37 The Nakagami probability density function for a number of different values of m.

value of the power received under Rayleigh fading conditions typically has a lognormal distribution. In other words, the Rayleigh distribution essentially is not a marginal distribution, but a conditional one:

$$f(a|\sigma) = \frac{a}{\sigma^2}\exp\left(-\frac{a^2}{2\sigma^2}\right)U(a), \tag{2.73}$$

where σ has the lognormal probability density function. The density function of the envelope can then be obtained as

$$f_A(a) = \int_0^\infty f(a|\sigma)f(\sigma)\,d\sigma, \tag{2.74}$$

resulting in the Suzuki distribution for the envelope of the received signal, given by

$$f_A(a) = \int_0^\infty \frac{a}{\sigma^2}\exp\left(-\frac{a^2}{2\sigma^2}\right)\frac{1}{\sqrt{2\pi}\sigma a}\exp\left[-\frac{(\ln\sigma-\mu)^2}{2\sigma^2}\right]d\sigma\,. \tag{2.75}$$

Once again, even though the Suzuki distribution is a more complete model, the fact that the pdf is not available in analytical form makes it a little difficult to work with.

2.4.5 Summary of Fading

The various fading mechanisms and the attenuation described can be summarized in a diagram as shown in Figure 2.38.

Note that Rician and Rayleigh fading arise out of multipath effects, and Nakagami fading can represent them both. This is not shown in the figure. For most cases, analyses based on Rayleigh or Rician fading are sufficient for understanding the nature of the mobile channel. A number of recent publications have suggested the use of Nakagami fading models to provide a generalized view of fading in wireless systems.

2.5 TESTING OF FADING MODELS

We have stated that the probability density functions of envelopes under various fading scenarios can be derived assuming certain fundamental conditions such as the existence of a multipath, the availability of a direct path, or the existence of multiple reflections. It is possible to conduct statistical tests to verify that the probability density function of the envelope of the faded signal follows a Rayleigh, Rician, or Nakagami distribution. One such test is the chi-square (χ^2) test (Papo 1991). The χ^2 test is a nonparametric (i.e., results are not dependent on the specific shape or parameters of the distribution) means of testing hypotheses (Papo 1991). Comparisons are made between theoretical populations based on assumed models and the actual data. The parameters of the expected theoretical probability density functions can be obtained from the data to estimate the theoretical probabilities.

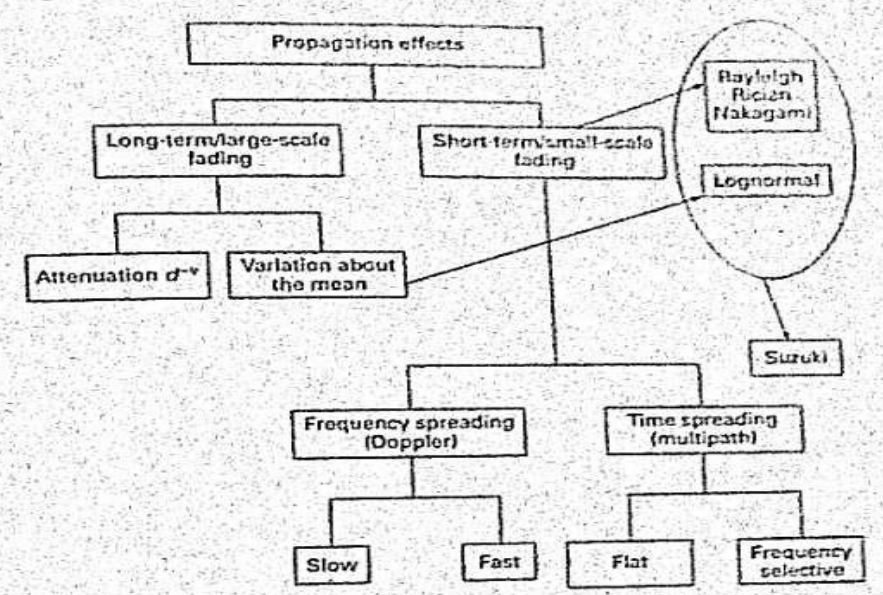

FIGURE 2.38 Overview of attenuation and fading. All forms of fading are shown along with their origins and relationships.

There are two major steps in χ^2 testing. First, a value is defined and calculated to estimate the difference between the expected theoretical frequency of occurrence and the experimentally observed frequency of occurrence. Second, this value is compared with a threshold to determine if it is too high. The threshold is determined by the significance level of the test selected by the investigator. The tests are conducted as follows:

1. Partition the observed sample space (N samples) into K disjoint intervals.
2. Calculate the number m_i of samples that fall in each of these intervals. This is a measure of the probability that the outcomes will fall in that interval.
3. Calculate the theoretical probability, p_i, that the outcomes would fall in the intervals. Thus, theoretically one expects Np_i samples to fall in the ith interval.

The χ^2 statistic is defined as the "weighted square error" and is given by

$$\chi^2 = \sum \frac{(\text{observed frequency} - \text{theoretical frequency})^2}{\text{theoretical frequency}} \tag{2.76}$$

$$= \sum_{i=1}^{K} \frac{(m_i - Np_i)^2}{Np_i}.$$

The test is good if the χ^2 statistic value is very small. The goodness of fit is quantified by setting a threshold X_T for the χ^2 statistic. We reject the hypothesis that the pdf indeed is the theoretical one if the value obtained in eq. (2.76) is larger than X_T.

The threshold is determined by the significance of the test. The test is based on the fact that when N is large, χ^2 has approximately a chi-square probability density function with $K-1$ degrees of freedom. The chi-square probability density function, $f(x)$, of a random variable X is given by

$$f(x) = \frac{x^{(K-2)/2}}{2^{K/2}\Gamma(K/2)} \exp\left(-\frac{x}{2}\right) U(x). \tag{2.77}$$

The pdf given in eq. (2.77) has $K-1$ degrees of freedom. The threshold, X_T, is selected so that

$$\text{prob}(X \geq X_T) = \alpha, \tag{2.78}$$

where α is the significance level represented by the shaded area in Figure 2.39. Typical values of α are 1% and 5%.

If parameters such as the mean and standard deviation of the expected theoretical density functions are computed from the data, the degrees of freedom are reduced by the number of parameters computed. For example, if the mean is computed from the data, the number of degrees of freedom goes down from $K-1$ to $K-1-1$. If r parameters are computed from the data, the degrees of freedom of the chi-square distribution will be $K-r-1$. In effect, each estimated parameter decreases the number of degrees of freedom by 1.

Table 2.1 gives values of the threshold for the chi-square test for significance levels of 5% and 1%.

We will now look at some examples of the use of the chi-square test.

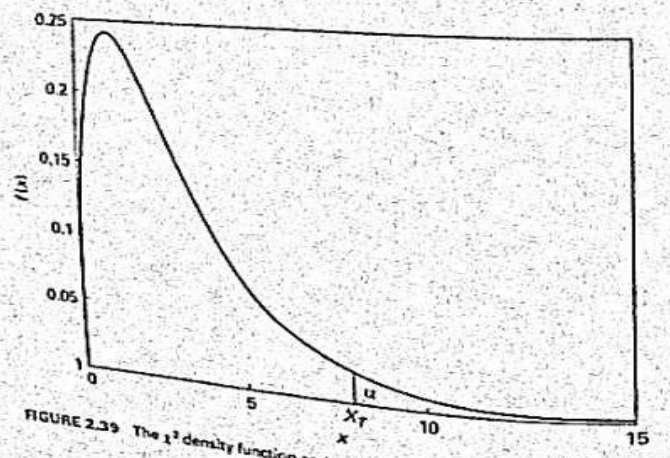

FIGURE 2.39 The χ^2 density function and the significance level.

TABLE 2.1 Chi-Square Values

K	X_T 5%	X_T 1%	K	X_T 5%	X_T 1%
1	3.84	6.63	15	25.00	30.58
2	5.99	9.21	16	26.30	32.00
3	7.81	11.34	17	27.59	33.41
4	9.49	13.28	18	28.87	34.81
5	11.07	75.09	19	30.14	36.19
6	12.59	16.81	20	31.41	37.57
7	14.07	18.48	22	33.90	40.30
8	15.51	20.09	24	36.40	43.00
9	16.92	21.67	25	37.65	44.31
10	18.31	23.21	26	38.90	45.60
11	19.68	24.73	28	41.30	48.30
12	21.03	26.22	30	43.80	50.90
13	22.36	27.69	40	55.80	63.70
14	23.68	29.14	50	67.50	76.20

EXAMPLE 2.11

Table 2.2 contains a set of numbers (100) given. Conduct a chi-square test to determine if these numbers are uniform in the range (0, 1).

TABLE 2.2 A Set of 100 Numbers

0.95	0.23	0.61	0.49	0.89	0.76	0.46	0.02	0.82	0.44
0.62	0.79	0.92	0.74	0.18	0.41	0.94	0.92	0.41	0.89
0.06	0.35	0.81	0.01	0.14	0.20	0.20	0.60	0.27	0.20
0.02	0.75	0.45	0.93	0.47	0.42	0.85	0.53	0.20	0.67
0.84	0.02	0.68	0.38	0.83	0.50	0.71	0.43	0.30	0.19
0.19	0.68	0.30	0.54	0.15	0.70	0.38	0.86	0.85	0.59
0.50	0.90	0.82	0.64	0.82	0.66	0.34	0.29	0.34	0.53
0.73	0.31	0.84	0.57	0.37	0.70	0.55	0.44	0.69	0.62
0.79	0.96	0.52	0.88	0.17	0.98	0.27	0.25	0.88	0.74
0.14	0.01	0.89	0.20	0.30	0.66	0.28	0.47	0.06	0.99

Let us pick a bin number of 10. If we now count the numbers in the bins (0 to 0.1, 0.1 to 0.2, etc.), bin 1 contains seven numbers, bin 2 contains seven numbers, and so on. If the numbers are uniformly distributed, $p_i = 0.1$. Hence $Np_i = 100 \times 0.1$. Note that for a uniform distribution, all the p_i are equal.

Therefore,

$$\chi^2 = \frac{(7-10)^2}{10} + \frac{(7-10)^2}{10} + \frac{(11-10)^2}{10} + \frac{(10-10)^2}{10} + \frac{(11-10)^2}{10} + \frac{(9-10)^2}{10} + \frac{(11-10)^2}{10} + \frac{(10-10)^2}{10} + \frac{(15-10)^2}{10} + \frac{(9-10)^2}{10} = 4.8. \tag{2.79}$$

From Table 2.1, $X_T(K-1) = X_T(9) = 16.92$ for $\alpha = 5\%$, which is obviously larger than the χ^2 value of 4.8 in this case. Therefore, the hypothesis that the numbers are uniform is accepted. □

EXAMPLE 2.12

Consider the set of numbers given in Table 2.3. We will test whether these samples follow a Rayleigh distribution.

TABLE 2.3 A Set of Numbers

2.53	5.52	1.99	1.19	2.33	2.43	2.38	2.01	2.00	0.83
2.43	2.56	3.17	4.37	2.45	0.24	3.11	2.70	0.56	2.53
0.64	2.53	2.74	3.33	1.48	2.97	3.64	3.69	2.68	1.72
1.90	1.46	2.57	3.03	2.64	3.25	3.29	2.77	2.58	0.35
3.23	1.76	2.34	4.11	1.95	2.00	0.66	2.27	4.67	2.41
2.64	1.24	1.40	3.59	1.22	1.55	0.78	3.67	1.21	2.70
0.94	1.92	2.19	3.95	1.37	2.11	1.52	4.27	0.28	3.46
2.33	3.20	0.77	1.43	3.59	2.51	0.62	1.06	2.89	1.02
1.56	1.76	2.33	4.67	2.75	2.10	2.69	1.68	3.51	0.68
3.20	1.43	4.12	1.51	3.83	2.02	2.76	1.21	2.89	2.29

Note that if these samples are Rayleigh distributed, the average of the squares of these samples should correspond to $2\sigma^2$, i.e.,

$$\langle A^2 \rangle = 2\sigma^2 \tag{2.80}$$

First we will compute this value. It is approximately equal to 6.6. This also means that the degrees of freedom will have to be reduced by 1. Once again, we will use 10 bins.

Since the largest value is 5.52, the bins will be in steps of 0.5 starting with 0.5. We can also compute the probabilities p_i ($i = 1, 2, \ldots, 10$) from the cumulative distribution function (CDF) of the Rayleigh distribution given by

$$F(a) = 1 - \exp\left(-\frac{a^2}{2\sigma^2}\right). \tag{2.81}$$

Table 2.4 gives the values of Np_i and m_i.

TABLE 2.4 Values of Np_i and m_i

Np_i	m_i
3.03	3
2.67	9
12.77	13
14.53	13
14.87	18
13.31	13
10.24	10
8.1	8
5.57	4
3.57	3

The chi-square test statistic can now be calculated using eq. (2.70), and we obtain a value of 3.93. From Table 2.1, the threshold value for acceptance for $\alpha = 5\%$ corresponds to $X_T(10-1-1) = X_T(8) = 15.51$, which is larger than 3.93, so we accept the hypothesis that the numbers are Rayleigh distributed. ■

EXAMPLE 2.13

Let us see whether the numbers in Table 2.2 follow the Rayleigh distribution. We first estimate $2\sigma^2$. This is found to equal 0.358. Now we proceed as in Example 2.12, with the 10 bins going from 0.1 to 1, and calculate the theoretical probabilities and the frequency from the data. This information is provided in Table 2.5.

TABLE 2.5 Values of Np_i and m_i

Np_i	m_i
2.75	7
7.82	7
11.7	11
13.8	10
14.2	11
13.2	9
11.1	11
8.71	10
6.32	15
4.29	9

The test statistic can now be calculated using eq. (2.76); the value is equal to 27.5, which is larger than the threshold value of $X_T(8) = 15.51$ ($\alpha = 5\%$) from Table 2.1. We therefore reject the hypothesis that the numbers in Table 2.2 are Rayleigh distributed. ■

2.6 POWER UNITS

A discussion of loss calculations would be incomplete without explaining the difference between dBm and dB. Power (P_0) in milliwatts (mW) can be expressed in terms of dBm as

$$P_0(\text{dBm}) = 10 \log_{10}\left[\frac{P_0(\text{mW})}{1\ \text{mW}}\right]. \tag{2.82}$$

In other words, the power in dBm is an absolute measure of the power in mW. For example, 10 mW of power is 10 dBm, 1 W of power is 30 dBm, and 1 μW is −30 dBm. The unit dB, on the other hand, is the ratio of two powers in identical units. For example, if the average signal power is P_0 (mW) and the average noise power is P_n (mW), the signal-to-noise ratio (S/N) can be expressed as

$$(\text{S/N})\,\text{dB} = 10 \log_{10}\left[\frac{P_0(\text{mW})}{P_n(\text{mW})}\right]. \tag{2.83}$$

Thus, the signal-to-noise ratio expressed in dB carries information on how strong or how weak the signal is relative to the noise. For example, if the signal-to-noise ratio is 0 dB, the signal power and noise power are equal. If the signal-to-noise ratio is 20 dB, the signal power is 100 times stronger than the noise power. If the

signal-to-noise ratio is −3 dB, the signal power is only 50% of the noise power. Note that dB expresses the ratio and therefore is not a measure of the absolute power. Because of this, we can write

$$\text{Transmit power (dBm)} - \text{receive power (dBm)} = \text{loss (dB)}. \quad (2.84)$$

2.7 SUMMARY

This chapter has presented the problems associated with the propagation of a wireless signal. The effects of attenuation were described using the Hata model. The fading phenomena were examined to explain the fluctuations in the received signal power. Based on the physics of propagation, the fading can be described in different terms, namely, short-term and long-term fading; slow and fast fading; frequency-selective and flat fading; and Rayleigh, Rician, lognormal, Nakagami, and Suzuki fading. Statistical testing of the hypotheses to validate the appropriate probability density function was also explained.

- Attenuation is a result of reflection, scattering, diffraction, and refraction of the signal by natural and human-made structures.
- The received power, P_r, is inversely proportional to (distance)$^\nu$, or $P_r \propto 1/d^\nu$, where ν is the loss parameter.
- The loss parameter ν is equal to 2 for free space and is in the range of 2–4 for different environments, being higher for urban areas and lower for rural areas.
- The loss in outdoor areas can be modeled using the Hata model or Lee's model.
- Indoor propagation models are based on the characteristics of the interior of the building, building materials, and other factors and are described in terms of various zone models.
- The random fluctuations in the received power are due to fading.
- Multipaths and the Doppler effect contribute to short-term fading, and multiple reflections lead to long-term fading.
- Short-term fading can be described using Rayleigh statistics if no direct path exists between the transmitter and the receiver.
- Short-term fading can be described using Rician statistics if there is a direct path between the transmitter and the receiver.
- Rician and Rayleigh statistics can be encompassed by a single distribution, the Nakagami distribution.
- Short-term fading due to a multipath not only causes random fluctuations in the received power, but also distorts the pulses carrying the information.
- The multipath-fading channel can be modeled by treating the channel as a low-pass filter.
- If the bandwidth of the channel is higher than the bandwidth of the message, the signal is characterized by "flat fading" and no pulse distortion. If the bandwidth of the channel is less than the bandwidth of the message, the result is a "frequency-selective fading" channel. This flat or frequency-selective behavior can be quantitatively described in terms of the rms delay by taking the power of each multipath and the corresponding time delay.

- The bandwidth of the channel or the coherence bandwidth of the channel is inversely proportional to the rms delay.
- If there is relative motion between the transmitter and receiver (i.e., the MU is moving), the result is Doppler fading. If the maximum Doppler shift is less than the data rate, there is a "slow" fading channel. If the Doppler shift is larger than the data rate, there is a "fast" fading channel.
- In general, the worst performance occurs in fading channels that are fast and frequency-selective.
- In addition to fast and frequency-selective fading, a channel may also experience problems due to random frequency modulation. This arises from the $\cos(\theta_i)$ term in eq. (2.51), which makes the equation correspond to FM. By virtue of the fact that θ_i is random and fluctuates with time, random frequency modulation occurs, which will lead to increased bit error rates (see Chapter 5).
- Both short-term and long-term fading lead to outage. The system goes into outage when the signal-to-noise ratio or the received power falls below the threshold set for optimal performance.
- Long-term fading is modeled using lognormal distribution. If the received power is expressed in dBm, the long-term statistical fluctuations are Gaussian distributed.
- To prevent the system from going into outage, a margin is included in the power budget. This is the difference between the ideal threshold needed to maintain acceptable performance and a practical threshold that is set above the ideal threshold by a few dB. This power difference constitutes the *power margin*.
- The Suzuki model incorporates the short-term fading (Rayleigh) and long-term fading (lognormal) into a single distribution. This is based on the property that the average power in Rayleigh fading itself is random and can be described using the lognormal distribution.
- The statistics of fading may be verified using the chi-square test.

PROBLEMS

Most of these problems require MATLAB.
**** Asterisks refer to problems better suited for graduate-level students.*

1. Using MATLAB, generate plots similar to the ones shown in Figure 2.6 to demonstrate the path loss as a function of the loss parameter for distances ranging from 2 km to 40 km. Calculate the excess loss (for values of $\nu > 2.0$) in dB.

2. The base station antenna is transmitting a power of 1 W. The transmitter antenna gain is unity while the receiver gain is 2. The system loss factor is unity (i.e., no loss). Find the received power in dBm at a distance of 5 km from the transmitter operating at 900 MHz in free space. (Hint: Use eq. (2.2))

3. Use MATLAB to plot the path loss predicted by the Hata model for the four separate environments. Assume a BS antenna height of 140 m, MU antenna height of 1.7 m, and a carrier frequency of 900 MHz.

4. Using the results of Problem 3 above, calculate approximately the loss exponent ν for the four separate cases.

5. Use MATLAB to generate the Rayleigh-faded signal shown in Figure 2.19. Use a carrier frequency of 900 MHz. (Hint: Use the concept of